Hybrid Compton-PET imaging for ion-range monitoring in hadron-therapy

J. Balibrea-Correa, C. Domingo-Pardo, I. Ladarescu, J. Lerendegui-Marco, I. Ladarescu, A. Tarifeño-Saldivia

IFIC (CSIC-UV)

C. Guerrero, M.C. Jimenez, J.M. Quesada, T. Rodriguez-González

University of Seville / Centro Nacional de Aceleradores

V. Babiano-Suarez, F. Calviño, M. Pallás

UPC-Barcelona

Thanks to the
Organizing committee
Antonio Fernández Prieto
Dolores Cortina Gil
Iris García Rivas
José Benlliure Anaya
Pablo Cabanelas Eiras
Pablo Vázquez Regueiro

PET monitoring, pros & cons

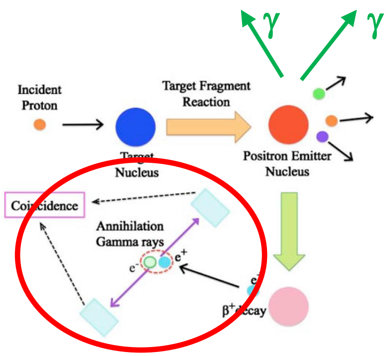

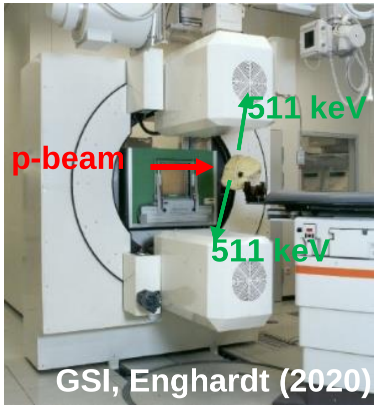

→ Range verification via PET (Llacer, 1979)

- Delayed (biological washout, organ motion…)
- Not directly coinciding with the Bragg peak
- Low counting statistics (10 Bq/ml) → Low efficiency
- Sensitive to tissue stoichiometry and mass density
- Functional character: physiological processes and tumour RF
- Excellent sensitivity (**1.3 mm, 50ms, 10^8p**) and tomographic functionality (KVI-Group, Siemens PET heads, ^{12}N, ^{13}O, b+ 10ms Ozoemelam 2020)

Dresden, Enghardt (2020)

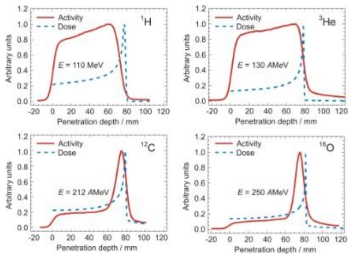

Prev. Talks by: Laura Moliner (I3M), Antoni Rucinski (CCB), A. Espinosa, C. Guerrero (USe)

Prompt-Gamma Imaging, pros &cons

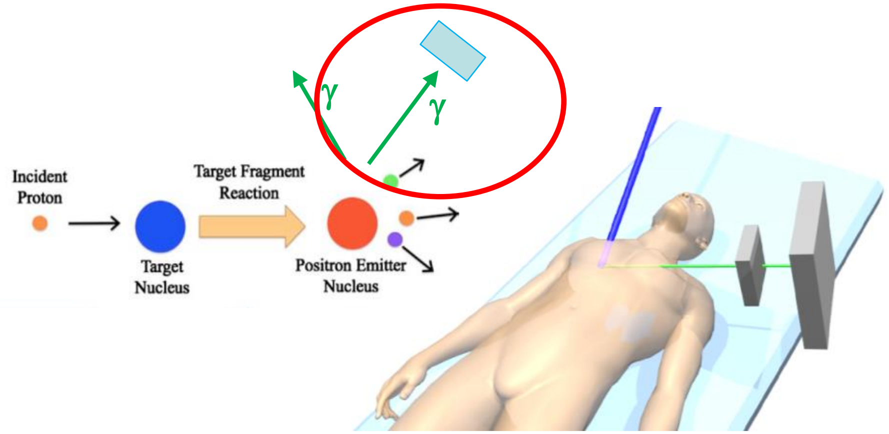

→ Range verification via Prompt Gamma Imaging (Stichelbault&Jongen, 2003)

- Most advanced electronic (Compton) imagers: Kabuki, 2009; Richard, 2012; Peterson, 2010; Kormoll, 2011; Llosa, 2013; etc
- High g-ray yield at the Bragg peak→reliable signature of the ion-range
- Limited intrinsic imaging resolution vs. PET → Still few mm range-shift feasible
- Low efficiency (particularly for more than two detection planes)
- Large neutron-induced backgrounds (in-beam)

Prev. Talks by G. Llosà (IFIC), P. Crespo (LIP)

PET monitoring, pros & cons

Prompt-Gamma Imaging, pros &cons

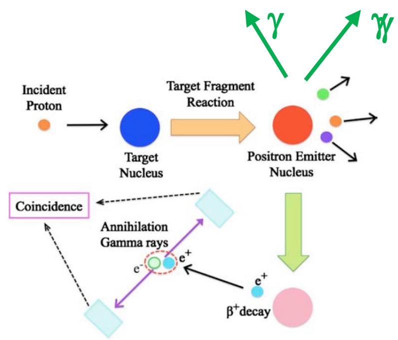

PET:

Delayed / Indirect

Efficiency

Image Resolution

Compton-PGI:

Prompt / Pristine

Efficiency

Signal/Background

Neutron backgrounds

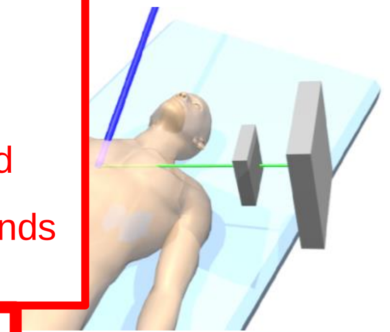

→ Range verification via PE

- Delayed (biological washout, or
- Not directly coinciding with the B
- Low counting statistics (10 Bq/m
- Sensitive to tissue stoichiometry
- Functional character: physiologi
- Excellent sensitivity (**1.3 mm, 5**
  functionality (KVI-Group, Sieme
  Ozoemelam 2020)

Dresden, Enghardt (2020)

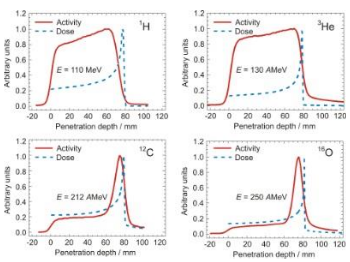

Pr
M
Ri
Es
(U

Compton PGI & PET together?

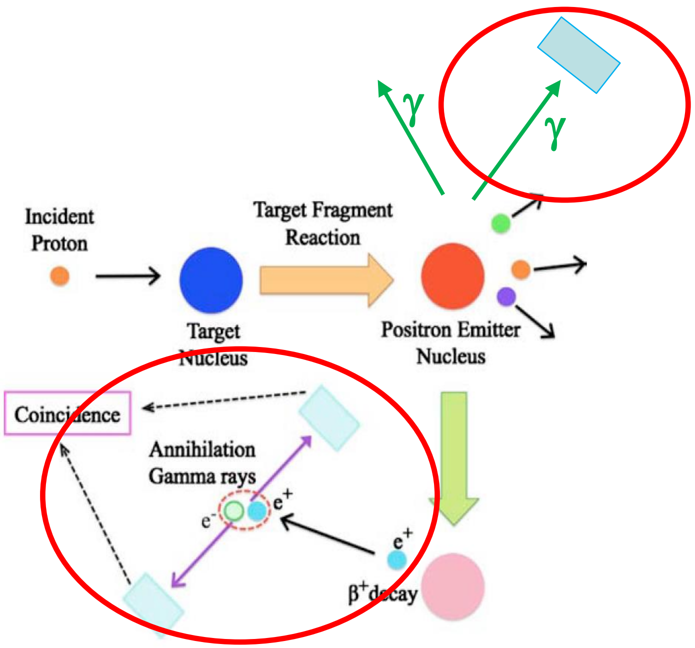

pt Gamma Imaging

n) imagers: Kabuki, 2009;
rmoll, 2011; Llosa, 2013; etc
→reliable signature of the

vs. PET → Still few mm

e than two detection planes)
ds (in-beam)

G. Llosà
po (LIP)

Hadron therapy: concept of hybrid Compton-PET imaging for ion-range verification

K. Parodi, Nucl. Instr. Meth. A (2016)

Nuclear Instruments and Methods in Physics Research A 809 (2016) 113–119

Contents lists available at ScienceDirect

Nuclear Instruments and Methods in Physics Research A

journal homepage: www.elsevier.com/locate/nima

On- and off-line monitoring of ion beam treatment

Katia Parodi

Ludwig Maximilians University, Department of Medical Physics, Am Coulombwall 1, 85748 Garching b. Munich, Germany

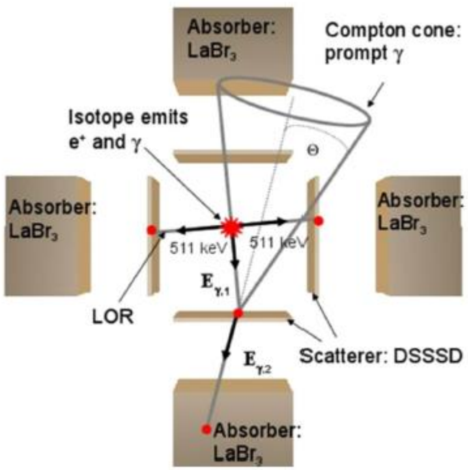

Fig. 3. Schematic illustration of the gamma-PET technique based on multiple Compton arms proposed in [58], which could be extended to hybrid operation by

(…) propose an original combination of different techniques in a **hybrid detection scheme**, aiming to **make <u>the most of complementary imaging methods and open new perspectives of image guidance for improved precision of ion beam therapy</u>.**

…novel concepts of **complementary PET and prompt gamma imaging** in a so called hybrid detection scheme. As already observed in [58], a possible solution would be a combination of multiple Compton camera arms offering sufficient solid angle over- age and using opposite single detector layers to serve as Compton camera scatterers or PET coincidence identifiers, complemented by additional absorbers for Compton imaging or total energy check in PET operation (Fig. 3). …

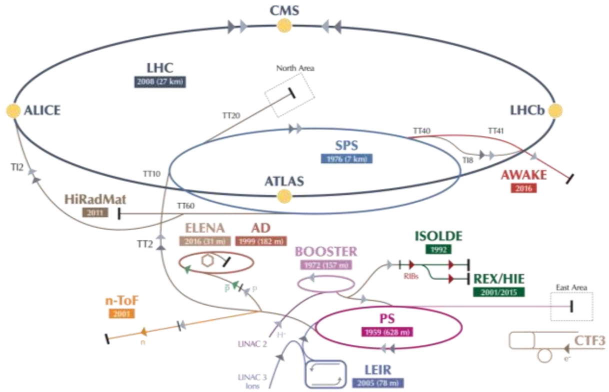

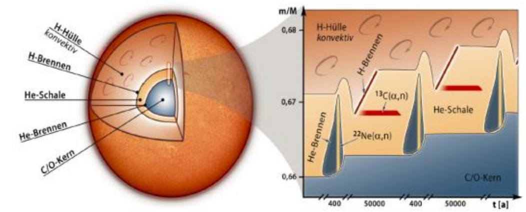

Nuclear Instruments and Methods in Physics Research A 825 (2016) 78–86

Contents lists available at ScienceDirect

Nuclear Instruments and Methods in Physics Research A

journal homepage: www.elsevier.com/locate/nima

i-TED: A novel concept for high-sensitivity (n,γ) cross-section measurements

C. Domingo-Pardo

Instituto de Física Corpuscular, CSIC-University of Valencia, Spain

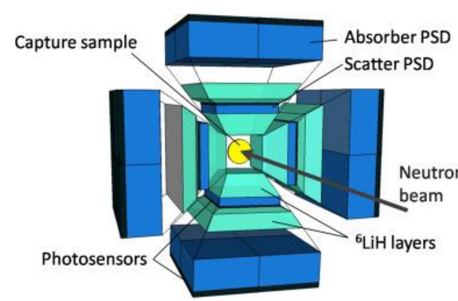

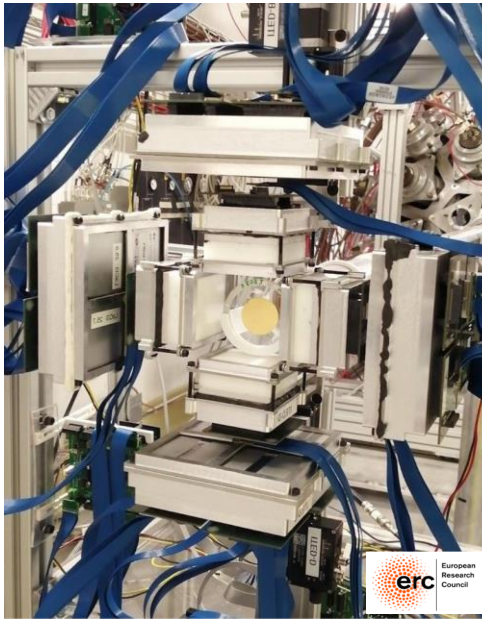

- High detection efficiency (500 cm^2 PSDs) → Online real-time range verification
- Low sensitivity to n-induced backgrounds ($LaCl_3$, ^{6}LiPE) → Improved S/B-ratio
- Good performance in the g-ray energy range up to 5-6 MeV (thick crystals)
- Compact & lightweight (TOFPET-ASICs) → Compatible with clinical environment

HYMNS ERC-CoG https://cordis.europa.eu/project/id/681740

Hadron therapy: concept of hybrid Compton-PET imaging for ion-range verification

K. Parodi, Nucl. Instr. Meth. A (2016)

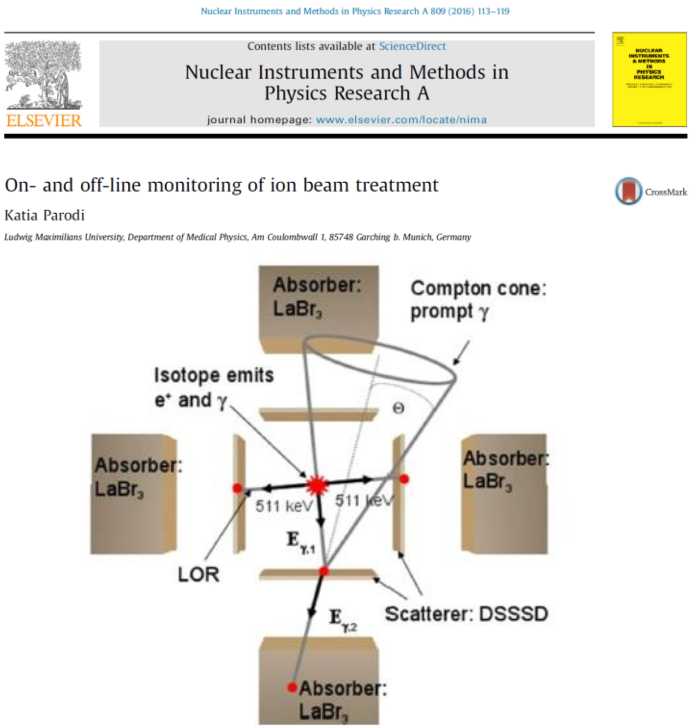

Nuclear Instruments and Methods in Physics Research A 809 (2016) 113–119

Contents lists available at ScienceDirect

Nuclear Instruments and Methods in Physics Research A

journal homepage: www.elsevier.com/locate/nima

On- and off-line monitoring of ion beam treatment

Katia Parodi

Ludwig Maximilians University, Department of Medical Physics, Am Coulombwall 1, 85748 Garching b. Munich, Germany

Fig. 3. Schematic illustration of the gamma-PET technique based on multiple Compton arms proposed in [58], which could be extended to hybrid operation by

(…) propose an original combination of different techniques in a **hybrid detection scheme**, aiming to **make <u>the most of complementary imaging methods and open new perspectives of image guidance for improved precision of ion beam therapy</u>**.

…novel concepts of **complementary PET and prompt gamma imaging** in a so called hybrid detection scheme. As already observed in [58], a possible solution would be a combination of multiple Compton camera arms offering sufficient solid angle over- age and using opposite single detector layers to serve as Compton camera scatterers or PET coincidence identifiers, complemented by additional absorbers for Compton imaging or total energy check in PET operation (Fig. 3). …

Applicable to ion-range monitoring in proton-therapy?

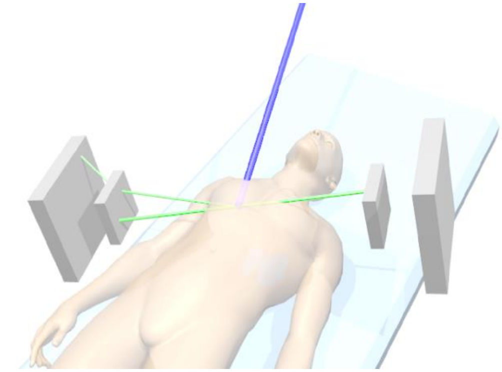

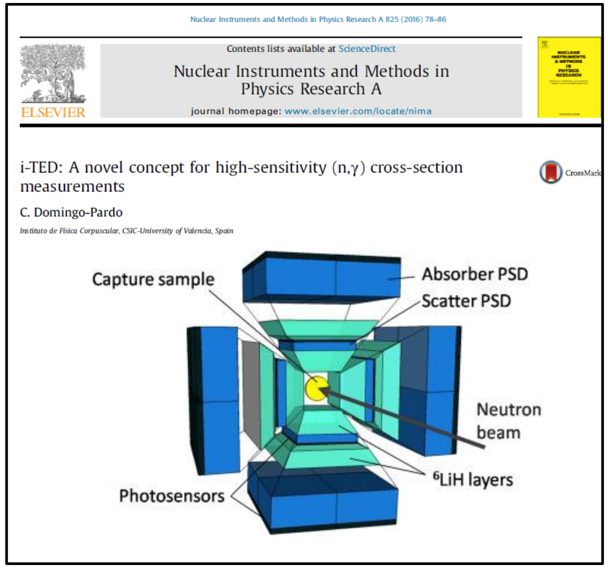

Nuclear Instruments and Methods in Physics Research A 825 (2016) 78–86

Contents lists available at ScienceDirect

Nuclear Instruments and Methods in Physics Research A

journal homepage: www.elsevier.com/locate/nima

i-TED: A novel concept for high-sensitivity (n,γ) cross-section measurements

C. Domingo-Pardo

Instituto de Física Corpuscular, CSIC-University of Valencia, Spain

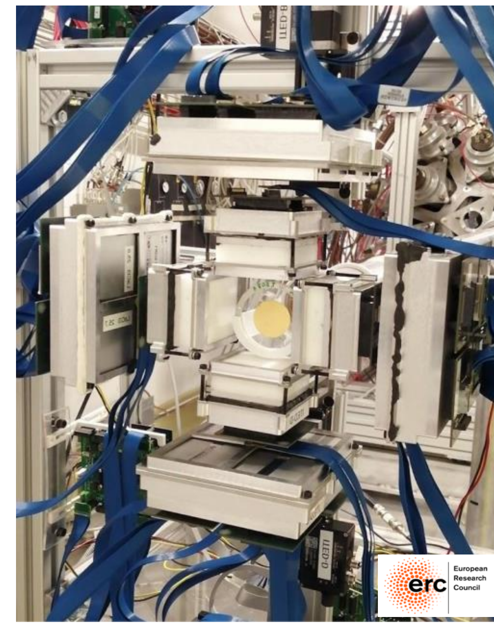

- High detection efficiency (500 cm^2 PSDs) → Online real-time range verification
- Low sensitivity to n-induced backgrounds (LaCl$_3$, ^{6}LiPE) → Improved S/B-ratio
- Good performance in the g-ray energy range up to 5-6 MeV (thick crystals)
- Compact & lightweight (TOFPET-ASICs) → Compatible with clinical environment

HYMNS ERC-CoG https://cordis.europa.eu/project/id/681740

Hadron therapy: concept of hybrid Compton-PET imaging for ion-range verification

J.Krimmer' Review on PGI, 2018:

Nuclear Inst. and Methods in Physics Research, A 878 (2018) 58-73

Contents lists available at ScienceDirect

Nuclear Inst. and Methods in Physics Research, A

journal homepage: www.elsevier.com/locate/nima

Prompt-gamma monitoring in hadrontherapy: A review

J. Krimmer [a], D. Dauvergne [b,*], J.M. Létang [c], É. Testa [a]

[a] IPNL, Université de Lyon, Université Lyon 1, CNRS/IN2P3 UMR5822, F-69622 Villeurbanne, France
[b] LPSC, Université Grenoble-Alpes, CNRS/IN2P3 UMR5821, F-38026 Grenoble, France
[c] Univ Lyon, INSA-Lyon, Université Claude Bernard Lyon 1, UJM-Saint Étienne, CNRS, Inserm, Centre Léon Bérard, CREATIS UMR 5220 U1206, F-69373, Lyon, France

2.3. Specificity of PG imaging

Table 2 presents the specificities of PG cameras for hadrontherapy with respect to conventional medical imaging. It is clear from these specificities that dedicated cameras are needed, with special features like high energy detection capability and count rate capability, and data acquisition systems that have to be adapted to the beam time structure.

For the particular objective of the precision for the falloff determination in the 1D-profile, the background plays a major role. Indeed, if we describe the falloff features in terms of contrast C, falloff width FW and background level B, it has been shown that the falloff retrieval precision FRP is determined by the following equation for homogeneous targets [32]:

$$FRP = \frac{\sqrt{B}}{C} = \frac{1}{\sqrt{N}} \qquad (1)$$

where N is the number of incident ions. A striking result is that the falloff width has no influence on the FRP. This means that the priority when optimizing camera designs is the detection efficiency and the background rejection (shielding, TOF,...).

As we will see in Section 4, detection efficiencies of PG cameras – ranging from 10^{-5} (collimated cameras) to 10^{-4} (Compton cameras) – will lead to relatively low numbers of detected PG at spot level for pencil beam scanning systems.

Applicable to ion-range monitoring in proton-therapy?

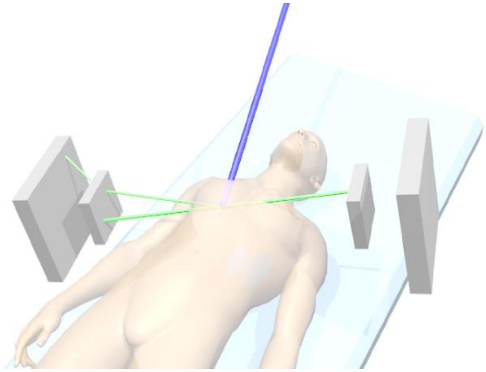

Nuclear Instruments and Methods in Physics Research A 825 (2016) 78–86

Contents lists available at ScienceDirect

Nuclear Instruments and Methods in Physics Research A

journal homepage: www.elsevier.com/locate/nima

i-TED: A novel concept for high-sensitivity (n,γ) cross-section measurements

C. Domingo-Pardo

Instituto de Física Corpuscular, CSIC-University of Valencia, Spain

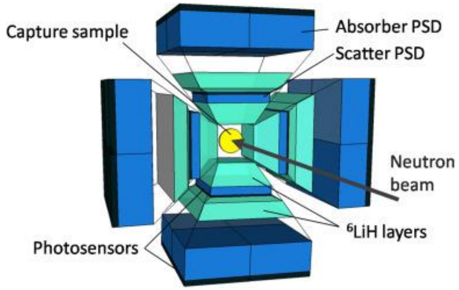

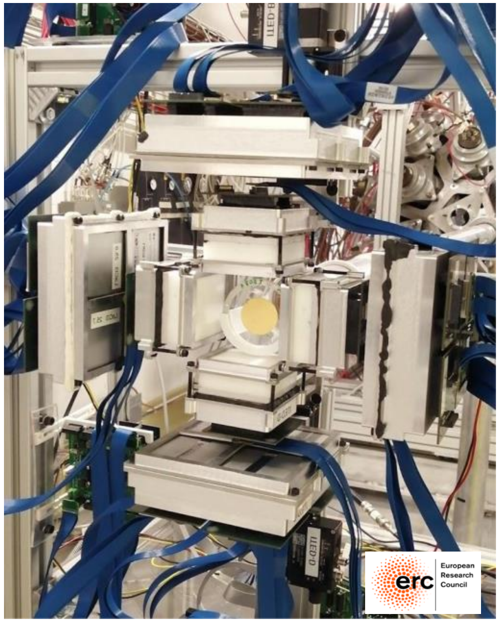

- High detection efficiency (500 cm^2 PSDs) → Online real-time range verification
- Low sensitivity to n-induced backgrounds ($LaCl_3$, ^{6}LiPE) → Improved S/B-ratio
- Good performance in the g-ray energy range up to 5-6 MeV (thick crystals)
- Compact & lightweight (TOFPET-ASICs) → Compatible with clinical environment

HYMNS ERC-CoG https://cordis.europa.eu/project/id/681740

i-TED Comtpon imagers applied to ion-range monitoring: A MC study


www.nature.com/scientificreports

scientific reports

Check for updates

OPEN Towards machine learning aided real-time range imaging in proton therapy

Jorge Lerendegui-Marco, Javier Balibrea-Correa, Víctor Babiano-Suárez, Ion Ladarescu & César Domingo-Pardo

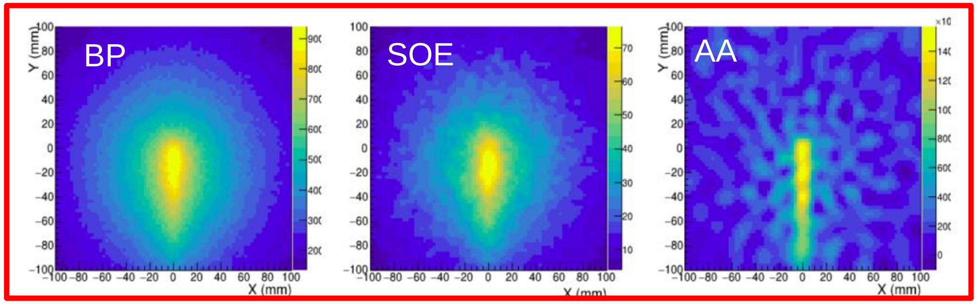

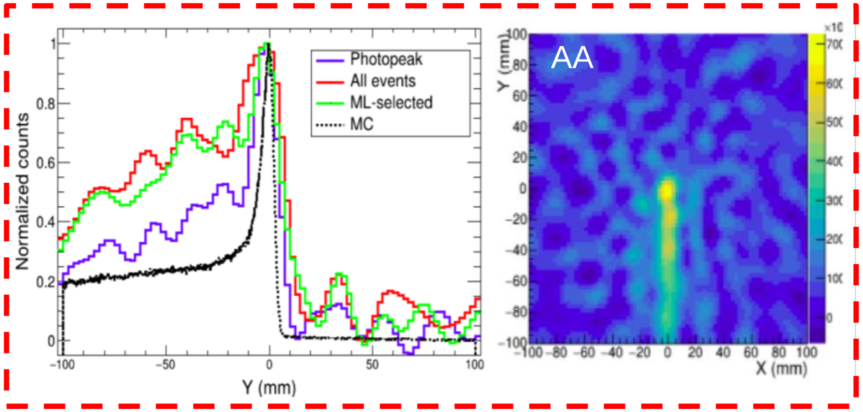

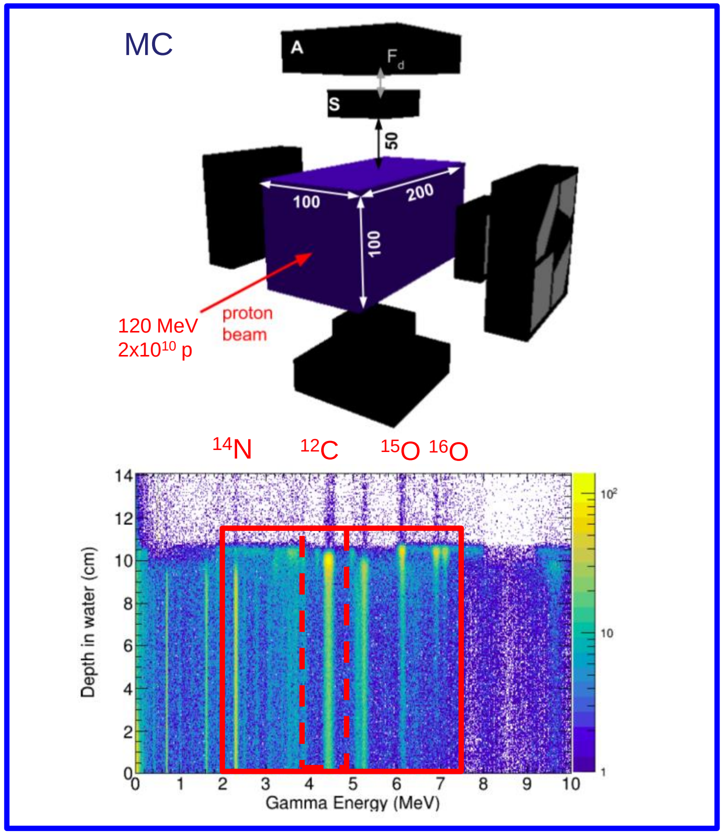

	Focal distance (mm)		
Energy selection	5	15	30
All PG (1-7 MeV)	2.6×10^{-4}	2.1×10^{-4}	1.6×10^{-4}
4 main PGs	4.3×10^{-5}	3.5×10^{-5}	2.6×10^{-5}
^{12}C (4.3-4.6 MeV)	1.5×10^{-5}	1.2×10^{-5}	8.8×10^{-6}

Algorithm	Time (s)
BP	<5
SOE	14
AA (CPU Single-thread)	1821
AA (CPU Multithreading-8)	260
AA (GPU)	15

Table: Efficiencies per incident proton at 10 cm from beam axis. E.g. x10^8 for total statistics/spot in realistic case.

J. Lerendegui-Marco, J. Balibrea-Correa, et al. (CDP), Scientific Reports (2022)

SOE: A. Andreyev et al., Phys. Med. Biol. 43 (2016)
AA: T. Tomitani et al. Phys. Med. Biol. 47 (2002)

Hybrid Compton-PET imaging: first Proof-of-Concept measurements at CNA-Seville

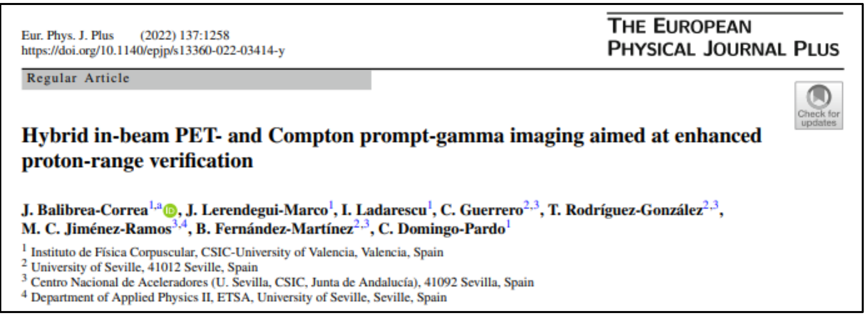
Eur. Phys. J. Plus (2022) 137:1258
https://doi.org/10.1140/epjp/s13360-022-03414-y
THE EUROPEAN PHYSICAL JOURNAL PLUS
Regular Article

Hybrid in-beam PET- and Compton prompt-gamma imaging aimed at enhanced proton-range verification

J. Balibrea-Correa[1,a], J. Lerendegui-Marco[1], I. Ladarescu[1], C. Guerrero[2,3], T. Rodríguez-González[2,3], M. C. Jiménez-Ramos[3,4], B. Fernández-Martínez[2,3], C. Domingo-Pardo[1]
[1] Instituto de Física Corpuscular, CSIC-University of Valencia, Valencia, Spain
[2] University of Seville, 41012 Seville, Spain
[3] Centro Nacional de Aceleradores (U. Sevilla, CSIC, Junta de Andalucía), 41092 Sevilla, Spain
[4] Department of Applied Physics II, ETSA, University of Seville, Seville, Spain

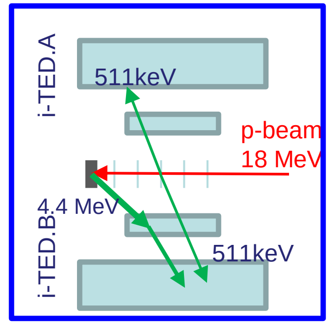

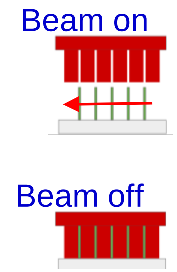

- 1 graphite layer (2mm)
- 5 layers of PMMA (100 μm)
- Beam off (PET of PMMAs)
- Beam on (CC Graphite)

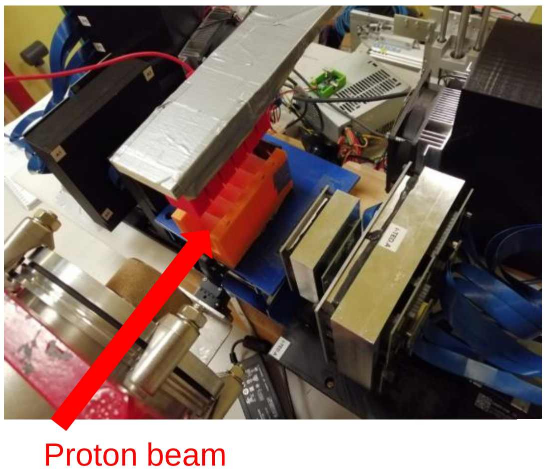

Centro Nacional de Aceleradores

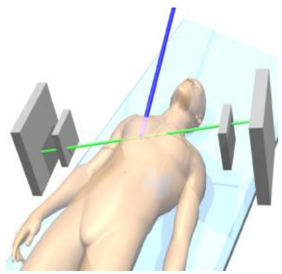

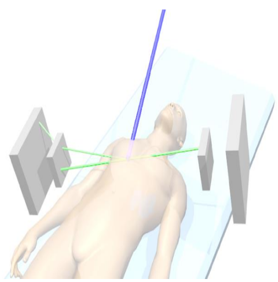

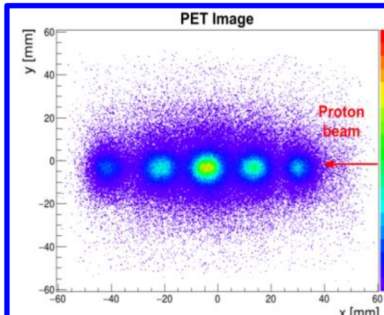

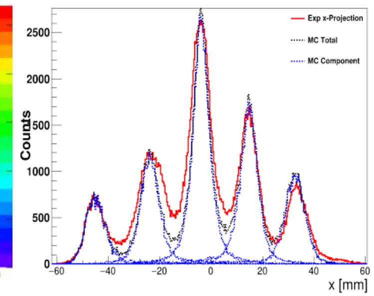

PET
Beam-off
PMMA layers
(100 μm)

Δx(PET) = 1 mm

6.4(6) mm FWHM

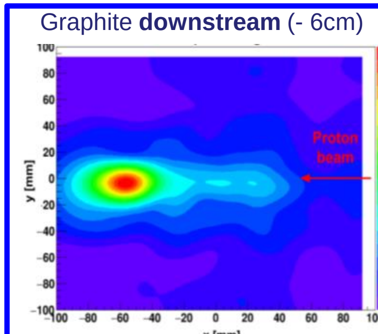

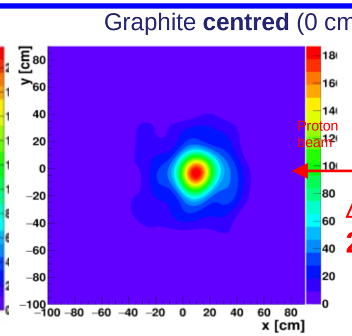

Compton
Eγ = 4.4 MeV
Beam-on
C-disk (2mm)

Δx(CC) = 1.2(9) mm
24.71(9) mm FWHM

→ First experimental demonstration of in-room hybrid Compton-PET concept with proton beams

J. Balibrea-Correa et al., Eur. Phys. Jour. Plus 137 (2022).

First hybrid Compton-PET imaging with i-TED in clinical conditions at HIT Heidelberg

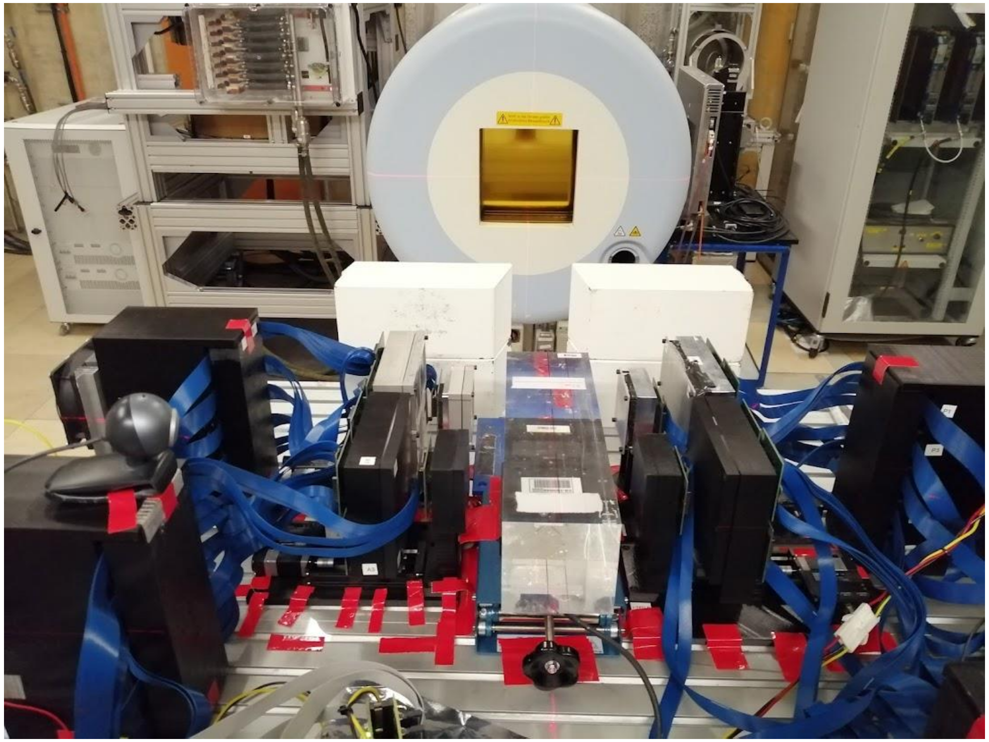

Heidelberg Hadrontherapy Center

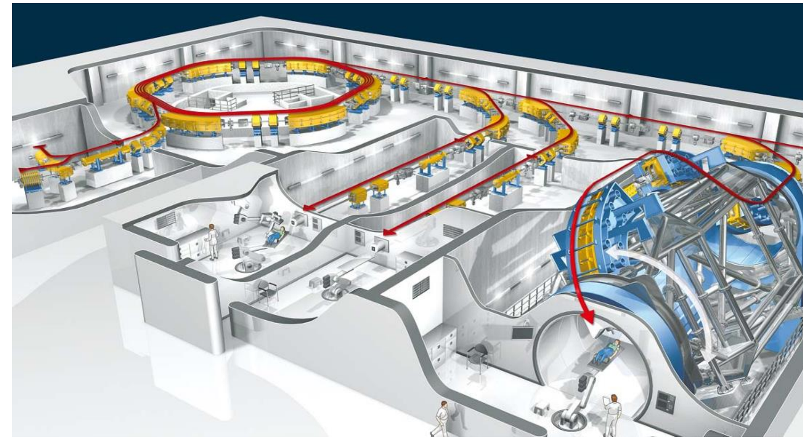

- → Clinical proton-beam energy (50-200 MeV)
- → Clinical proton-intensity ($2x10^9$ p/point)

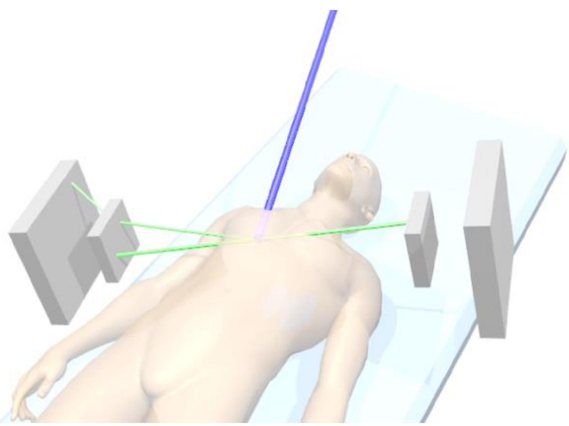

First hybrid Compton-PET imaging with i-TED in clinical conditions at HIT Heidelberg

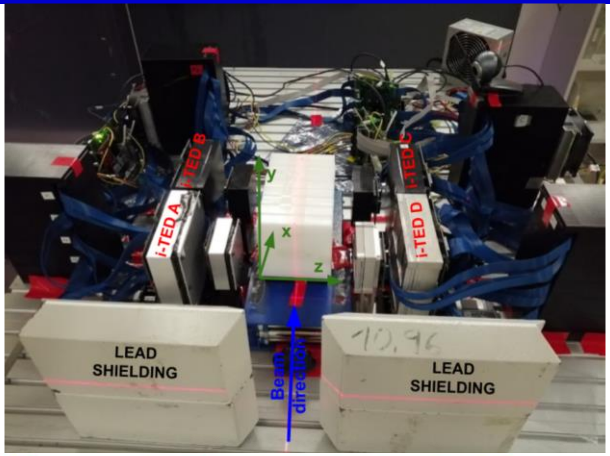

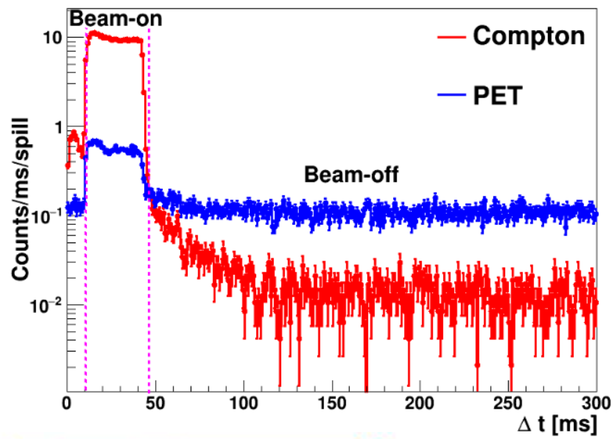

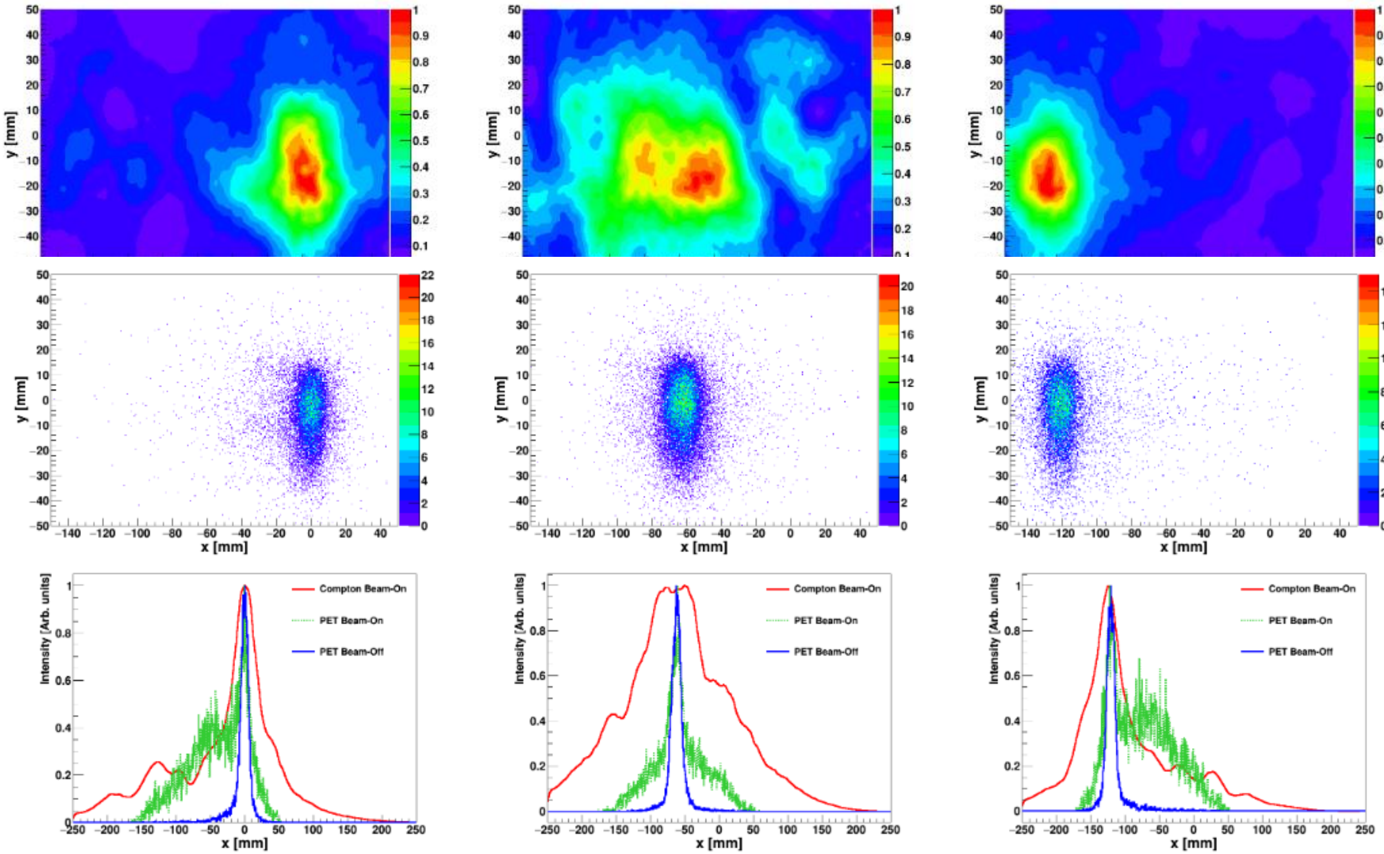

Compton

PET

Hybrid Compton-PET

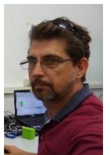

J. Balibrea-Correa, J. Lerendegui-Marco, et al. (HIT, USe) (publication in preparation)

Next steps: Hybrid Compton-PET and “multimessenger” approach: combining gamma-rays and neutrons MCIN-PDC2021-12536-C21

4x i-TED CCs in cross-config:

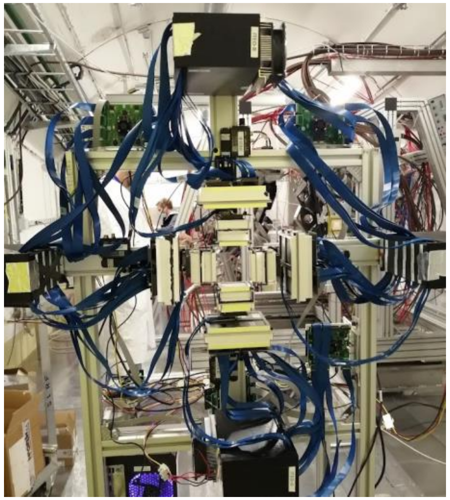

DACQ synchro LINrem & CC:

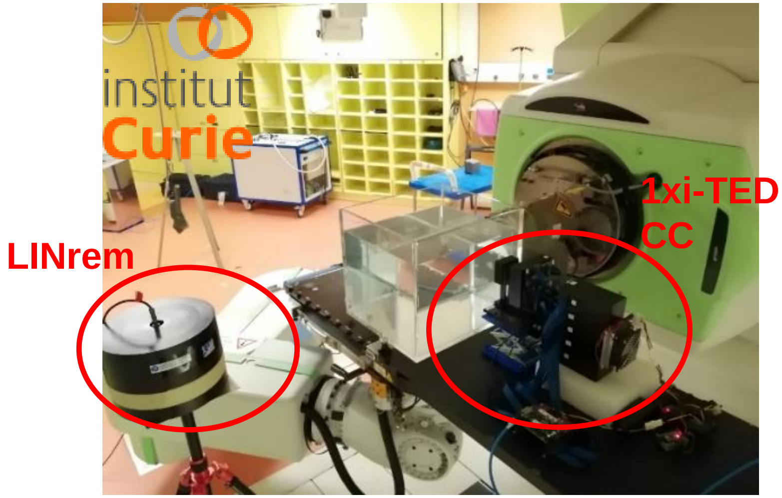

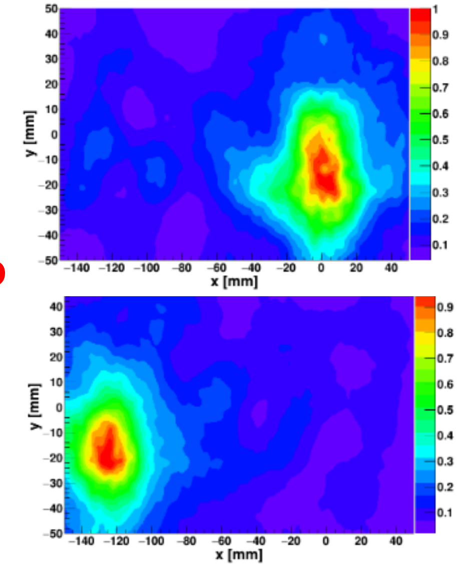

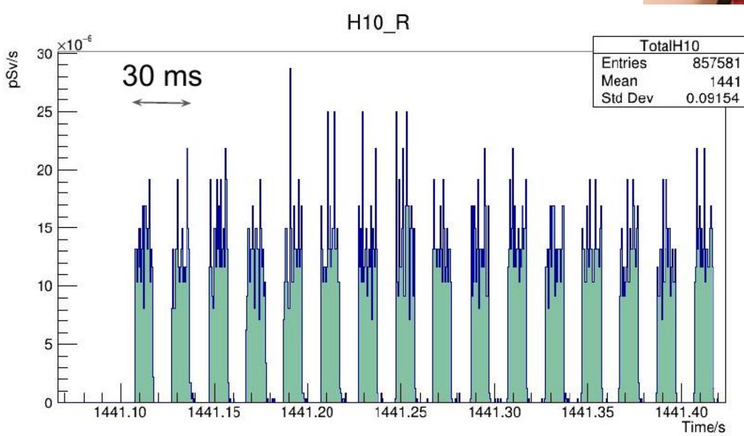

Prev. Talk by A. Tarifeño “Neutron dosimetry in particle therapy facilities: status of the LINrem project”

- Next measurements planned at Quironsalud, Madrid in july 2023,
- Future access to an **experimental proton-therapy room**, like the one foreseen at Santiago dC, would be an excellent opportunity!

ICPO

Collimator: Brass collimator 65mm thickness and 55 mm circular aperture

Phantom: 34×40×35 cm³ water phantom

Clinical dose: 3.5 Gy at the entrance of the phantom

Energies: 100, 150 and 200 MeV

Time structure: spots 10 ms width, 10 ms beam-off (approx)

Summary & Outlook

- We have developed an array of four Compton cameras optimized for high detection sensitivity and low neutron-induced backgrounds, whith potential applications in ion-range monitoring for proton-therapy treatments
- MC Simulations [Lerendegui22], as well as previous review studies (Krimmer'18) show the relevance of large efficiency and low neutron backgrounds to aim for real-time ion-range monitoring
- First proof-of-concept measurements for the hybrid Compton-PET approach [Parodi2016] have been carried out with two CCs in front-to-front configuration at the CNA cyclotron using 18 MeV proton beam, delivering excellent results for both PET and Compton imaging [Balibrea23]
- Measurements have been made with four CCs in front-to-front configuration at HIT Heidelberg, using p-, He- and C-beams at clinical energies and intensities. Data analysis is in progress and preliminary results are quite satisfactory.
- Next steps involve new measurements (in plan at Quironsalud in july 2023 at Madrid), thereby aiming at four CCs in cross-configuration and time-synchronization with ^{3}He-based neutron dosimeters (LINrem) for exploring the interplay between primary and secondary dose
- **A dedicated experimental proton-therapy room at Santiago de Compostela would be highly beneficial for future R+D+I works and developments!!!**

PDC2021-121536-C21

Backup slides

i-TED requirements for (n,γ) experiments **with enhanced S/B-ratio**

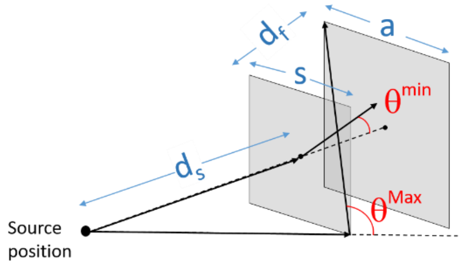

$$\delta\theta = \frac{E}{\sin\theta}\sqrt{\left(\frac{1}{E'^2}\left(\frac{\delta E'}{E'}\right)^2 + 2\sin^2\theta\left(\frac{\delta r}{r_{12}}\right)^2\right)}$$

$\Delta E/E$ = 3.5%

$\Delta E/E$ = 6.5%

Δr=1mm

Δr=3mm

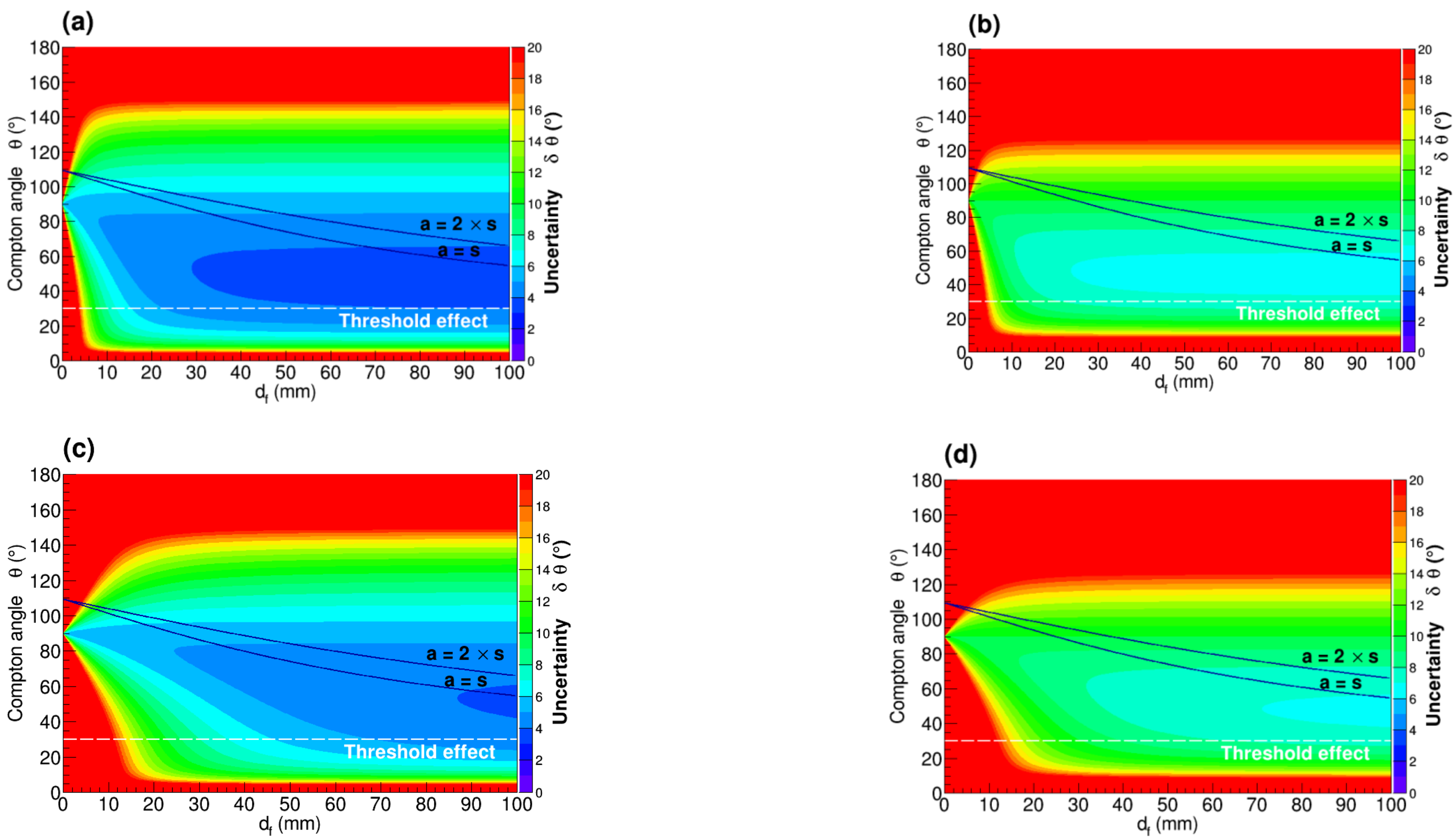

V.Babiano et al., NIM-A (2019)

SiPM
(sensL ArrayJ-30065-P-PCB)

LaCl3(Ce)
[White reflector]

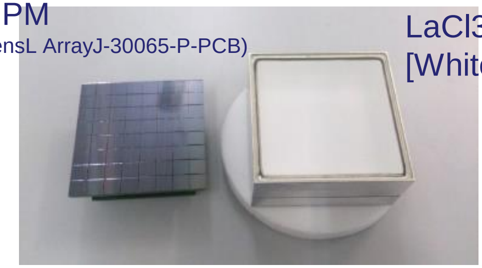

$\langle \Delta E/E \rangle$ = 4.5% @ 662keV

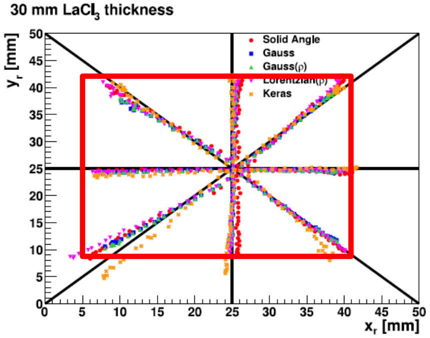

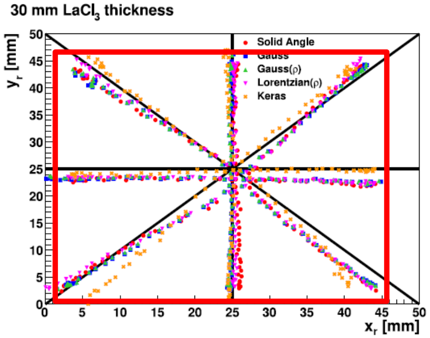

Support Vector Machine (linear kernel) Python sklearn-learn

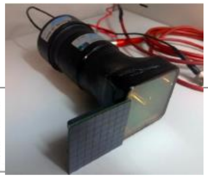

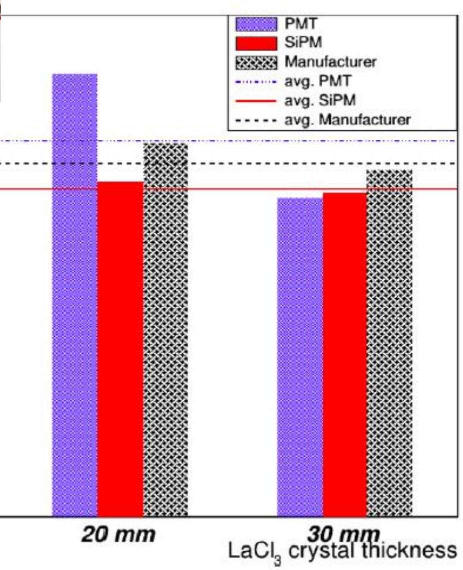

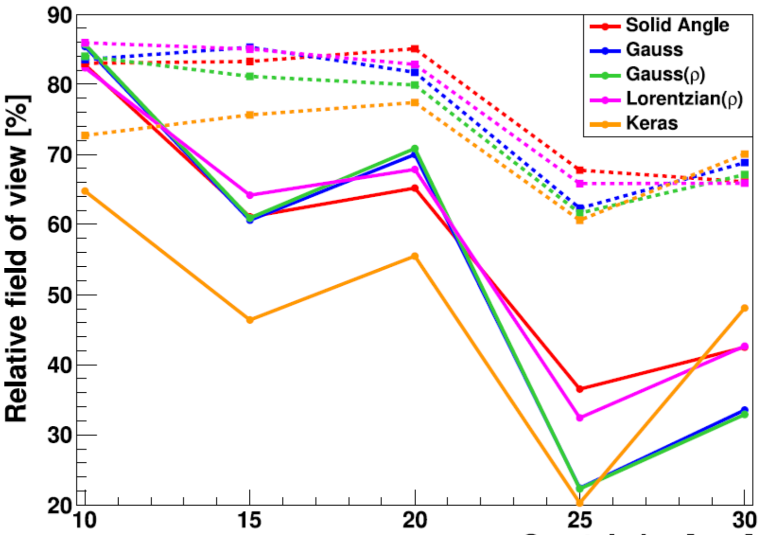

Size: 50x50 mm^2

P. Olleros et al., JINST 13-P03014 (2018)

P.Olleros, TFM@HYMNS, Avail. https://hymnserc.ific.uv.es

J. Balibrea-Correa et al. (CDP), NIM-A 1001 (2021) 165249

i-TED requirements for (n,γ) experiments **with enhanced S/B-ratio**

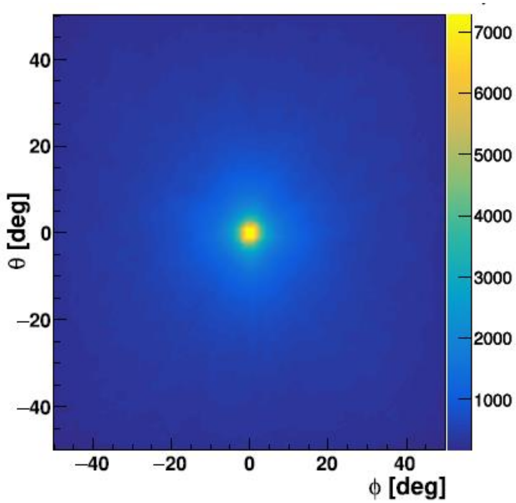

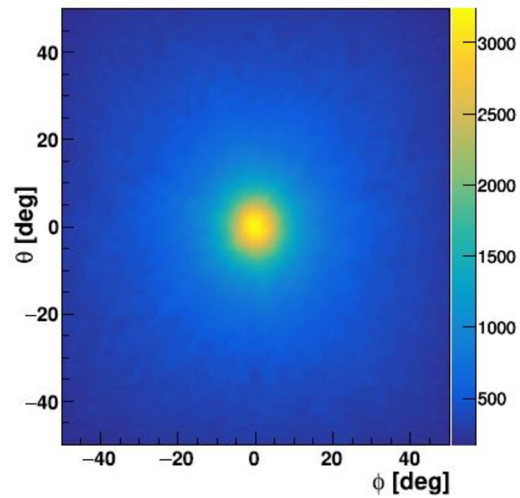

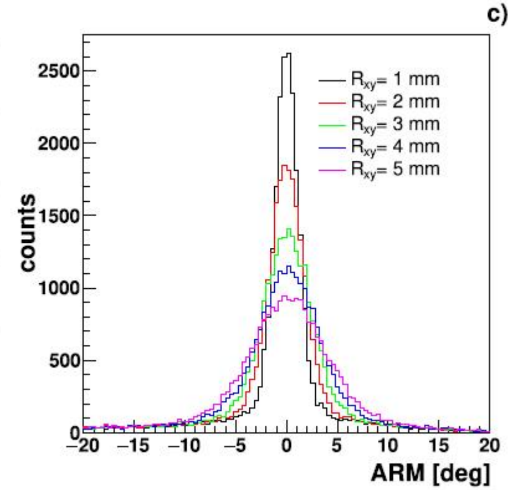

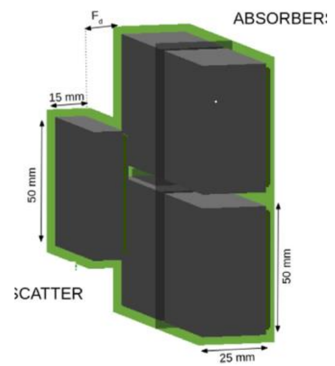

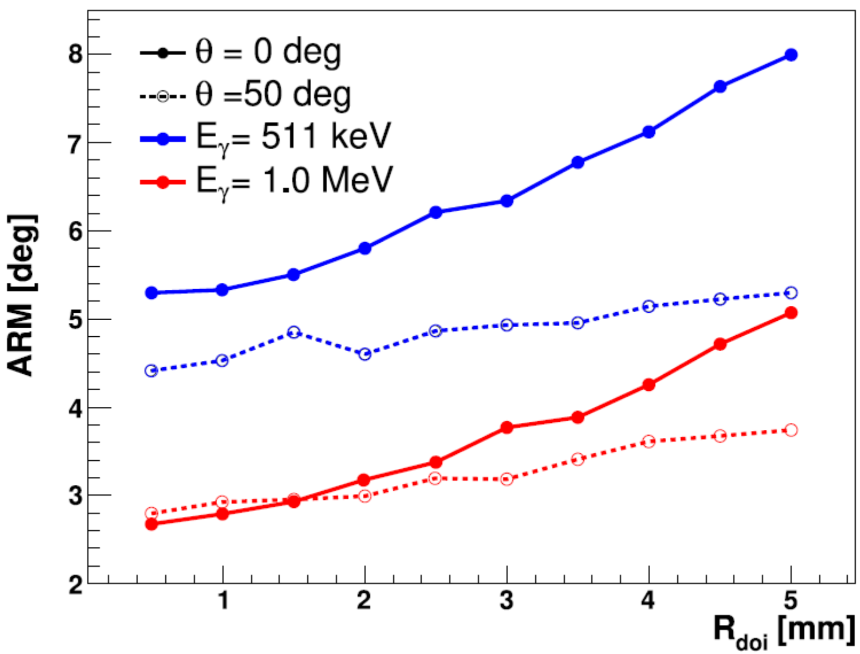

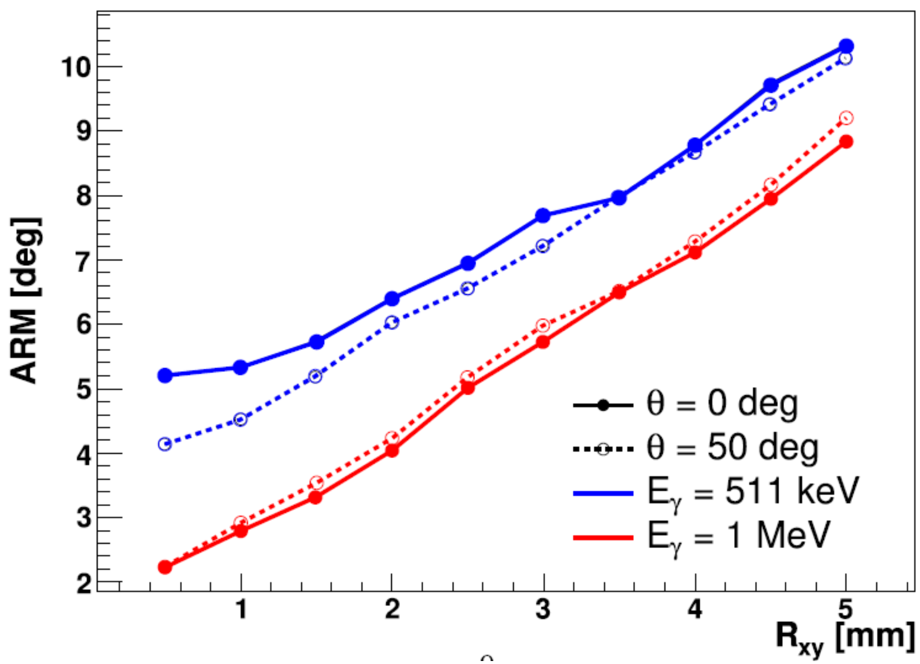

J. Balibrea-Correa et al. (CDP), NIM-A 1001 (2021) 165249

$$\cos(\theta) = 1 - \frac{m_e c^2 E_s}{(E_s + E_a)E_a}$$

Improved Compton imaging algorithms

Na-22 source, 1274 keV peak, i-TED @ 100 mm

Back-projection [1]
- Very Fast
- Poor resolution
- Poor peak to background

Analytical algorithm[2]
- Computational costly
- Improved resolution
- Huge improvement in peak/background

SOLUTION: GPU-BOOSTING
Back to computation times similar to BP

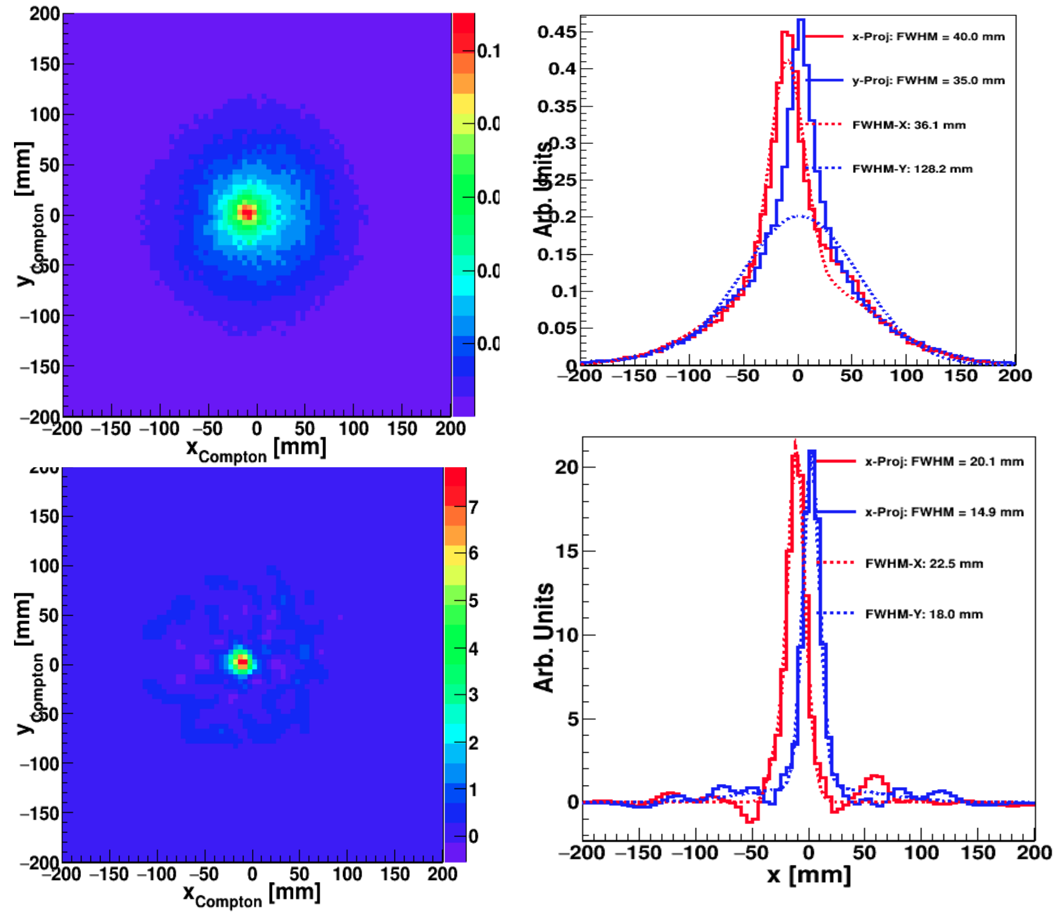

ARM(BP) = 11º → ARM(AA) = 5º

[1] Wilderman, S. J., et al. DOI:10.1109/NSSMIC.1998.773871 (1998)
[2] Tomitani et al., DOI: 10.1088/0031-9155/47/12/309 (2002)

i-TED: intrinsic position resolution Δr FWHM / DOI

DoI

reconstructed DoI coordinates for the central scan position

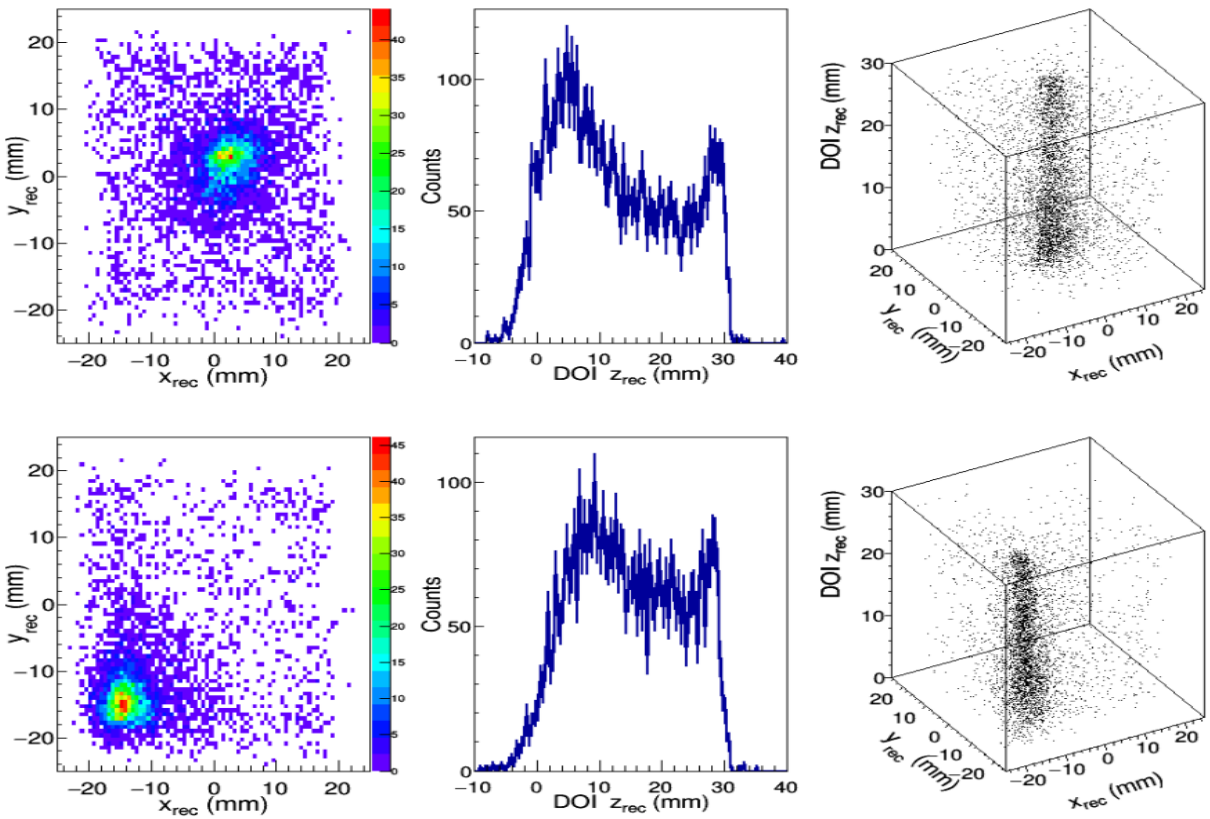

reconstructed DoI coordinates for a peripheral scan position

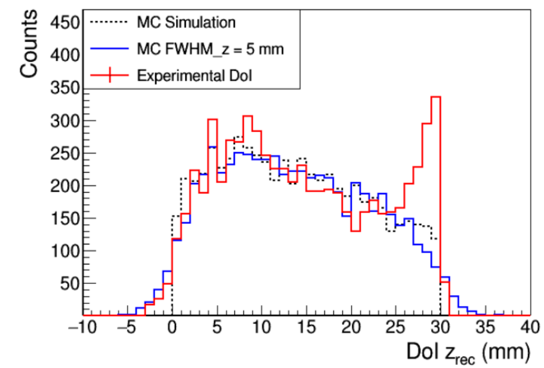

The measured values for Aw at half maximum (already calibrated) are compared against MC calculated DoIs and true or ideal simulated DoI values.

V.Babiano et al, NIM-A 931 (2019)

i-TED: intrinsic position resolution Δr FWHM / SUMMARY & COMPARISON

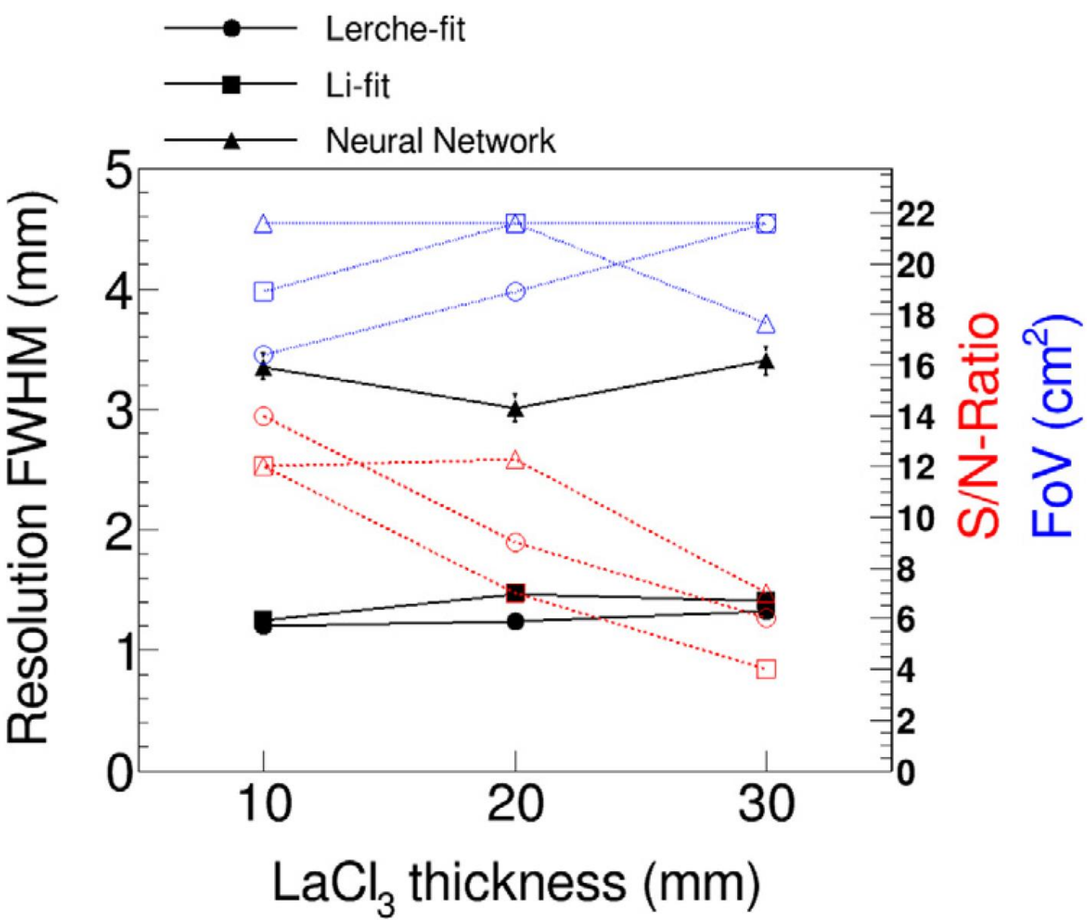

Model	Crystal size (mm^3)	Resolution $(\text{FWHM})_{x,y}$ (mm)	RMS $r_{rec} - r_{true}$ (mm)	FoV (cm^2)	S/N-ratio
Lerche	$50 \times 50 \times 10$	1.20(15)	0.84(19)	15.2	14(3)
	$50 \times 50 \times 20^a$	1.24(10)	0.69(8)	18.9	9(2)
	$50 \times 50 \times 30^a$	1.32(20)	0.86(13)	21.6	6(2)
Li	$50 \times 50 \times 10$	1.24(10)	0.86(23)	18.9	12(5)
	$50 \times 50 \times 20^a$	1.46(12)	0.67(4)	21.6	7(3)
	$50 \times 50 \times 30^a$	1.43(12)	0.88(16)	21.6	4(2)

Crystal size (mm^3)	Resolution $(\text{FWHM})_{(x,y)}$ (mm)	RMS $r_{rec} - r_{true}$ (mm)	FoV (cm^2)	S/N-ratio
$50 \times 50 \times 10$	3.35(11)	0.86(7)	21.6	12.0(2)
$50 \times 50 \times 20$	3.01(11)	0.83(6)	21.6	12.3(4)
$50 \times 50 \times 30$	3.4(11)	0.94(16)	17.6	7.0(4)

V.Babiano et al, NIM-A 931 (2019)

HYMNS: High sensitivitY Measurements of key stellar Nucleo-Synthesis reactions

European Research Council

YMNS

→Full i-TED = 4S+4A= 500 cm^2

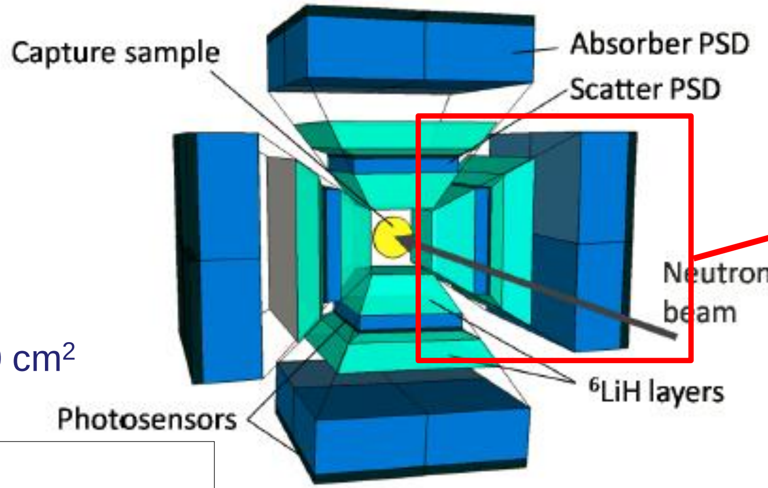

i-TED Demonstrator

Readout: 1280 channels (!)

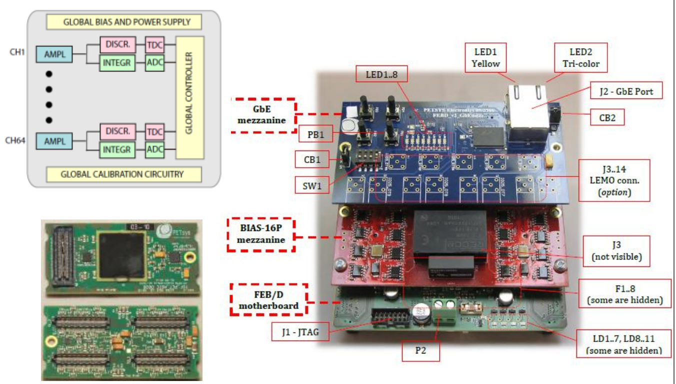

PETsys Electronics S.A. (Customized)

R.Bugalho et al., JINST_079P_0918

PSDs: 10 mm (S) and 25 mm (A)

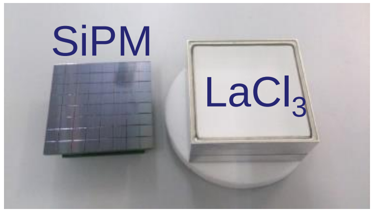

→ # pixels= 8x8y = 64 ch

→ pixel size **= 6x6 mm^2**

→ area = 5x5 cm^2 = 25 cm^2

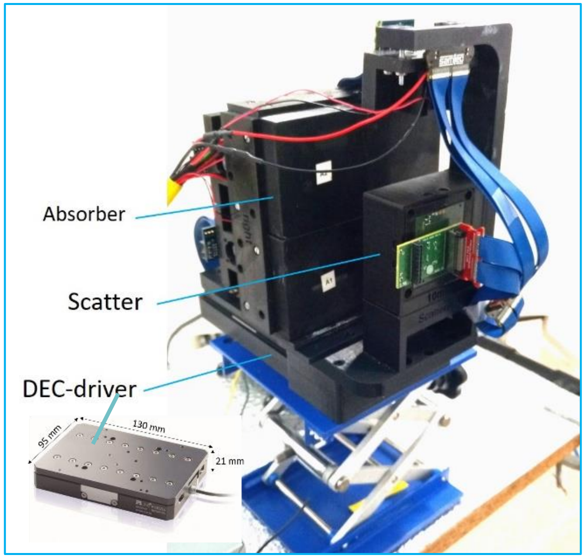

Patent PCT/ES2016/070916 "Focusable Compton Camera", 21/12/2016 - WO 2017/109256 AI (CDP et al.)

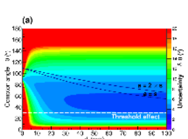

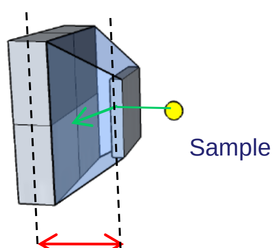

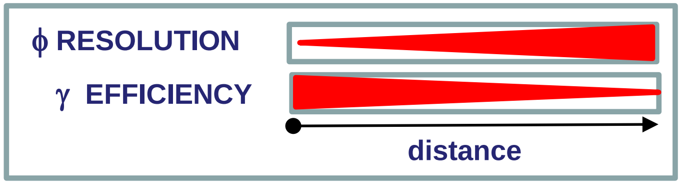

i-TED Total Energy Detector with γ-ray imaging capability

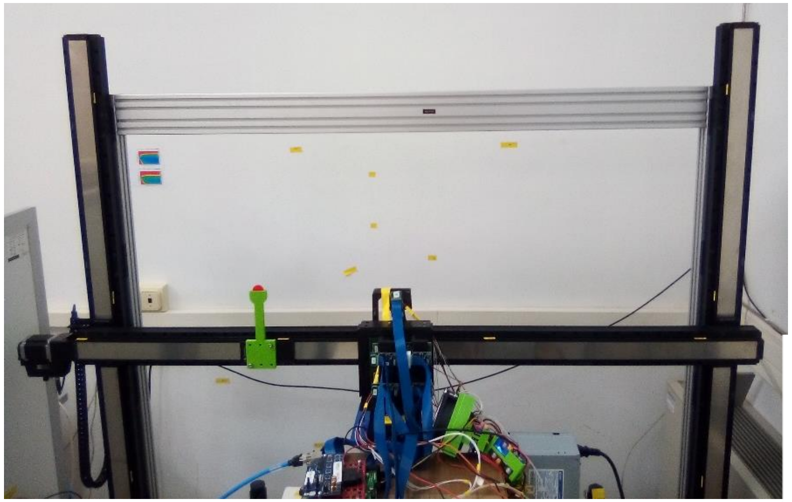

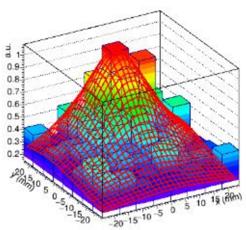

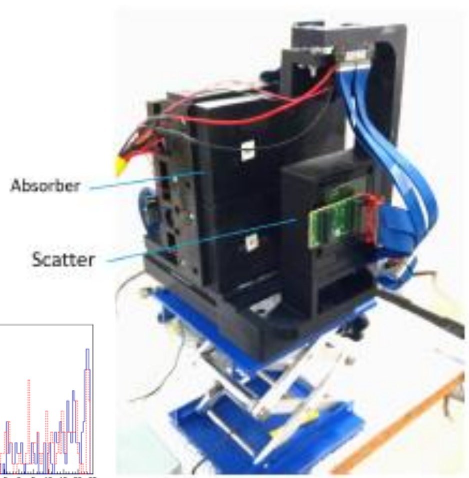

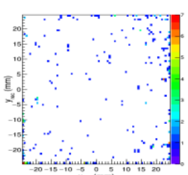

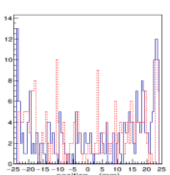

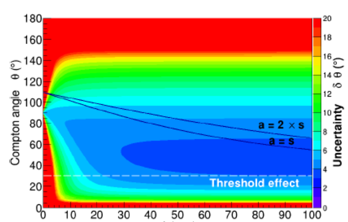

Back-projection Compton test:

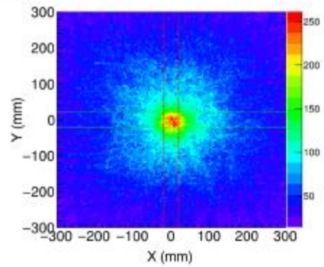

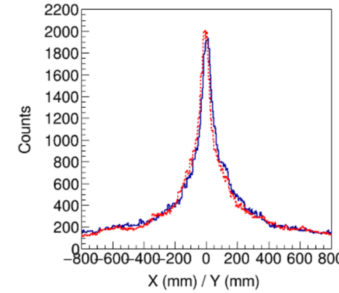

FoV: 2/3x2π sr

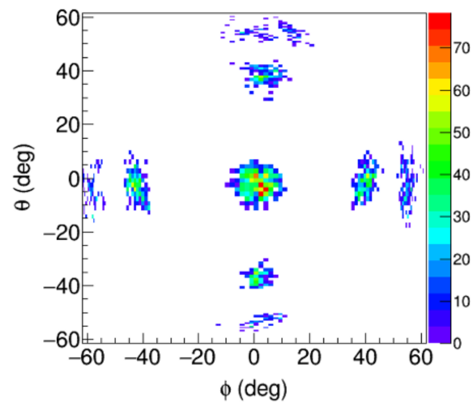

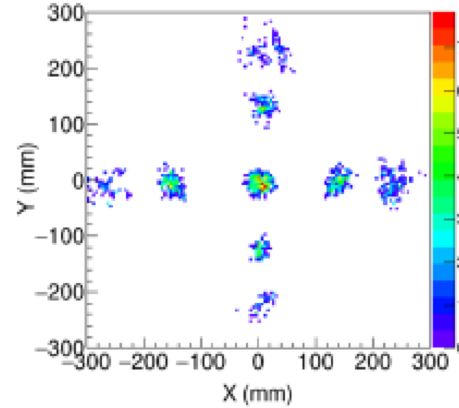

θ-resolution at 662 keV

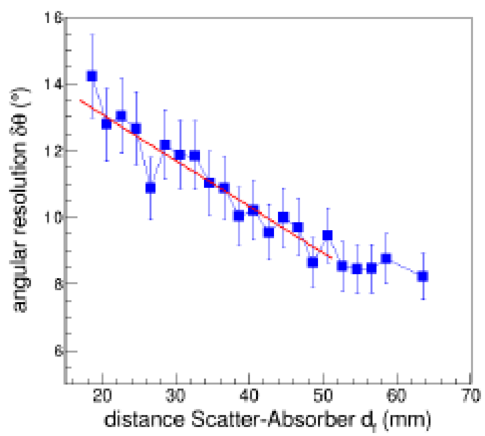

Efficiency at 662 keV

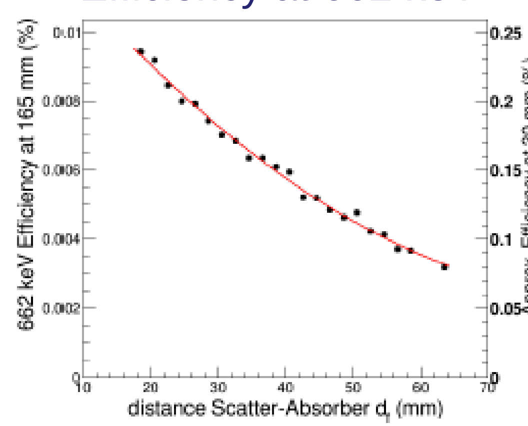

V.Babiano et al., NIM-A (in review, 2019)

i-TED applied to Hadron Therapy: A MC viewpoint

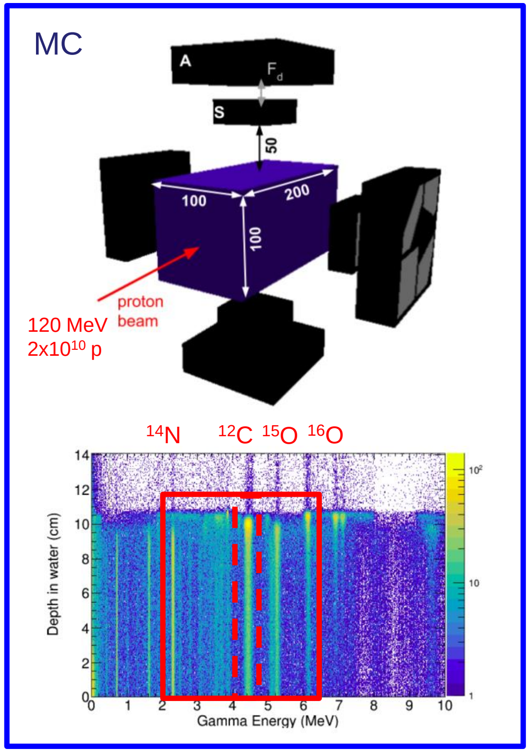

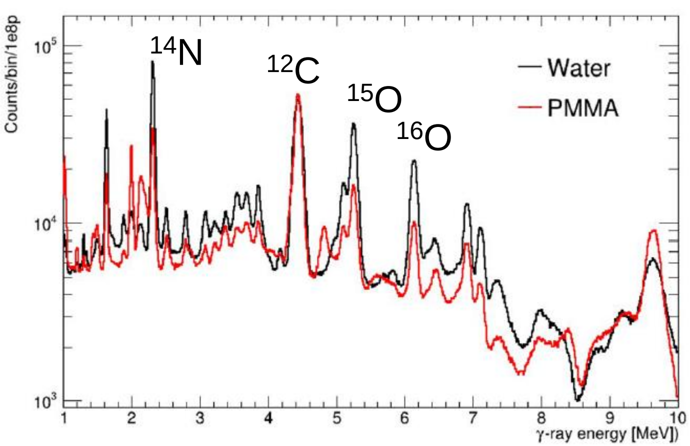

J. Lerendegui, J. Balibrea, et al. (CDP), Nat. Scientific Reports (2022)

Target	γ energy (MeV)	Assignments	Other data
^{16}O	1.89	^{16}O$(p, pp\gamma_{1.89})$ ^{15}N	
	2.0	^{16}O$(p, x\gamma_{2.04})$ ^{15}O	
		^{16}O$(p, x\gamma_{2.00})$ ^{11}C	
	2.31	^{16}O$(p, x\gamma_{2.31})$ ^{14}N	(Foley *et al* 1962)
			(Lang *et al* 1987)
	2.8	^{16}O$(p, p'\gamma_{2.74})$ ^{16}O	(Lang *et al* 1987)
		^{16}O$(p, x\gamma_{2.79})$ ^{14}N	(Kiener *et al* 1998)
		^{16}O$(p, x\gamma_{2.80})$ ^{11}C	
		^{16}O$(p, x\gamma_{2.87})$ ^{10}B	
	3.68	^{16}O$(p, x\gamma_{3.68})$ ^{13}C	
	4.44	^{16}O$(p, x\gamma_{4.44})$ ^{12}C	(Foley *et al* 1962)
			(Lang *et al* 1987)
			(Belhout *et al* 2007)
	5.2	^{16}O$(p, x\gamma_{5.24})$ ^{15}O	(Foley *et al* 1962)
		^{16}O$(p, pp\gamma_{5.27})$ ^{15}N	(Lang *et al* 1987)
		^{16}O$(p, x\gamma_{5.18})$ ^{15}O	(Belhout *et al* 2007)
		^{16}O$(p, pp\gamma_{5.30})$ ^{15}N	
	6.1	^{16}O$(p, p'\gamma_{6.13})$ ^{16}O	(Foley *et al* 1962)
		^{16}O$(p, x\gamma_{6.18})$ ^{15}O	(Narayanaswamy *et al* 1981)
			(Lang *et al* 1987)
			(Kiener *et al* 1998)
			(Belhout *et al* 2007)
	6.32	^{16}O$(p, x\gamma_{6.32})$ ^{15}N	
	7.0	^{16}O$(p, p'\gamma_{6.92})$ ^{16}O	(Foley *et al* 1962)
		^{16}O$(p, p'\gamma_{7.12})$ ^{16}O	(Kiener *et al* 1998)
^{12}C	2.0	^{12}C$(p, x\gamma_{2.00})$ ^{11}C	(Clegg *et al* 1961)
			(Lang *et al* 1987)
	2.1	^{12}C$(p, pp\gamma_{2.12})$ ^{11}B	(Lang *et al* 1987)
		^{12}C$(p, x\gamma_{2.15})$ ^{10}B	
	2.8	^{12}C$(p, x\gamma_{2.80})$ ^{11}C	
		^{12}C$(p, x\gamma_{2.87})$ ^{10}B	
	4.44	^{12}C$(p, p'\gamma_{4.44})$ ^{12}C	(Clegg *et al* 1961)
			(Lang *et al* 1987)
			(Kiener *et al* 1998)
			(Belhout *et al* 2007)
	4.80	^{12}C$(p, x\gamma_{4.80})$ ^{11}C	

J.M. Verburg, J.Seco, Phys. Med. Biol (2014)

i-TED applied to Hadron Therapy: A MC viewpoint

- High detection efficiency, high CR-capability → Real time
- Low sensitivity to n-induced backgrounds → Improved S/B-ratio
- Good E- and spatial resolution → Few mm accuracy
- Suitable performance in the gamma-ray energy range up to 5-6 MeV
- Compact & lightweight → Compatible with clinical environment

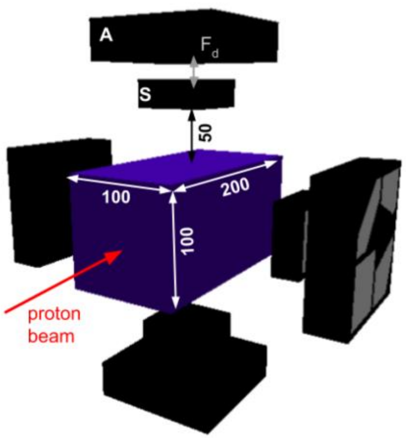

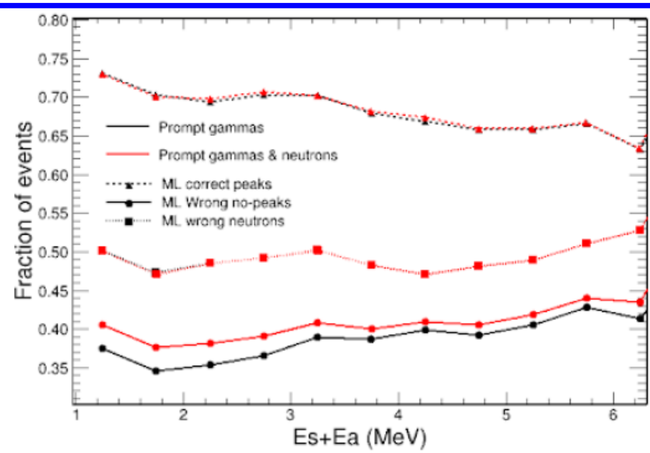

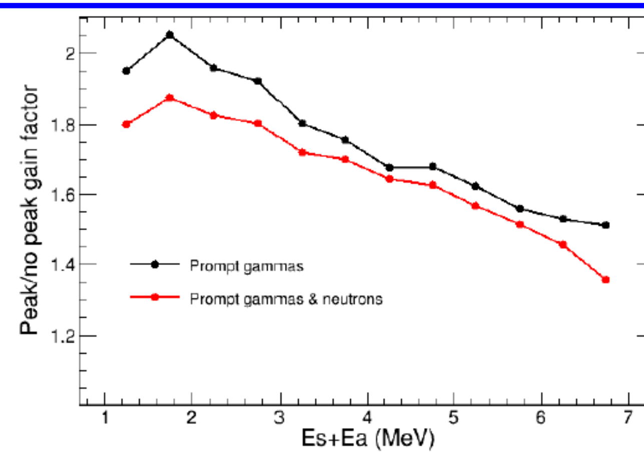

→Best ML algorithms Boosted Decision Trees (XGBoost) and ANN (Tensorflow), out of kNN, Logistic Regression, SVM, Gaussian Naive Bayes, RandomForest, AdaBoost and Quadratic Discriminant Analysis

→Trained with 5×10^{10} γ-rays in 200keV-7MeV Energy range, using r1(x1,y1,z1), r2(x2,y2,z2), E1, E2, Compton angle, KN-formula

→Classifier Output: 0 (Non FEE) or 1 (FEE)

→Accuracy between 65% (6MeV) and 73% (1MeV), Confussion: 35-40% of Non FEE predicted as FEE.

→S/N ratio enhanced between 1.5 and 2.1

→Capable of rejecting 50% of neutron events (neutron sensitivity)

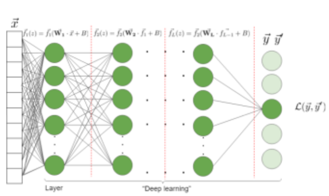

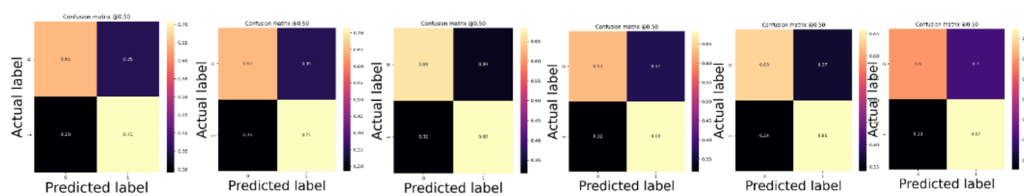

J. Lerendegui, J. Balibrea, et al. (CDP), Nat. Scientific Reports, 2021

Neutrons in HT: the role of a CC optimized for low neutron sensitivity

IOP Publishing — Physics in Medicine and Biology
Phys. Med. Biol. 57 (2012) 6429–6444 doi:10.1088/0031-9155/57/20/6429

Time-of-flight neutron rejection to improve prompt gamma imaging for proton range verification: a simulation study

Aleksandra K Biegun[1,6], Enrica Seravalli[2], Patrícia Cambraia Lopes[1,3,4], Ilaria Rinaldi[4,5], Marco Pinto[3], David C Oxley[6], Peter Dendooven[6], Frank Verhaegen[2], Katia Parodi[4], Paulo Crespo[3] and Dennis R Schaart[1]

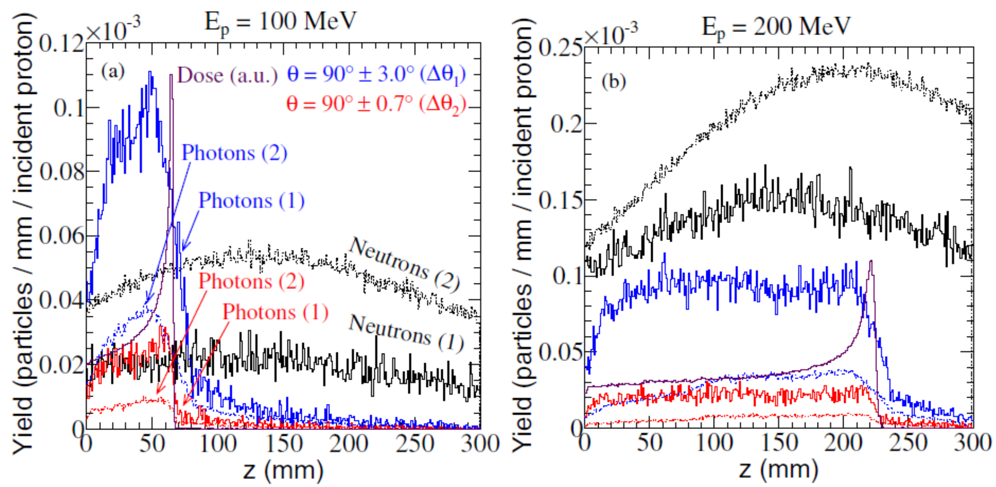

J. Krimmer et al. NIM-A (2018)

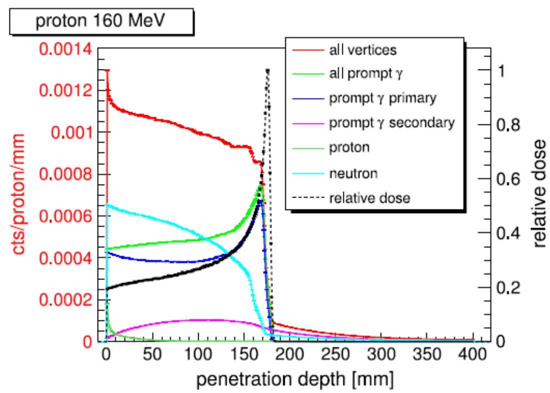

Fig. 1. Emission vertices of secondaries with energies larger than 1 MeV emerging from a water target (cylinder with 15 cm diameter, 40 cm length) irradiated by a 160 MeV proton beam.

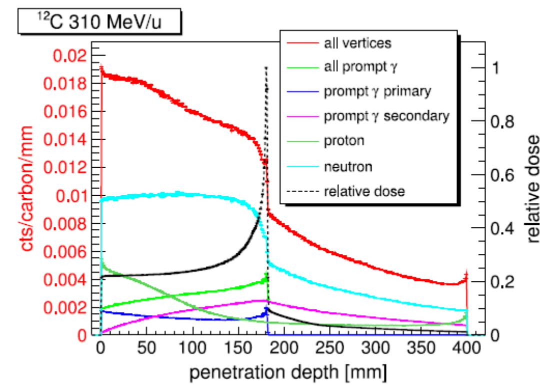

Fig. 2. Same as Fig. 1, for 310 MeV/u carbon ion beam.

i-TED applied to HT: A MC constrasted with neutron measurements at CNA-Seville

- High detection efficiency, high CR-capability → Real time
- **Low sensitivity to n-induced backgrounds** → Improved S/B-ratio
- Good E- and spatial resolution → Few mm accuracy
- Suitable performance in the gamma-ray energy range up to 5-6 MeV
- Compact & lightweight → Compatible with clinical environment

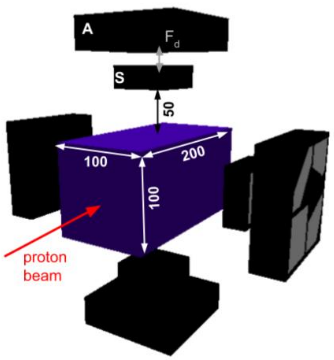

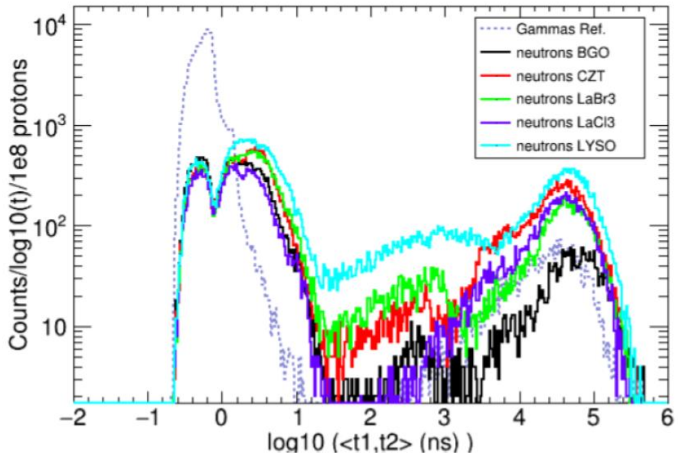

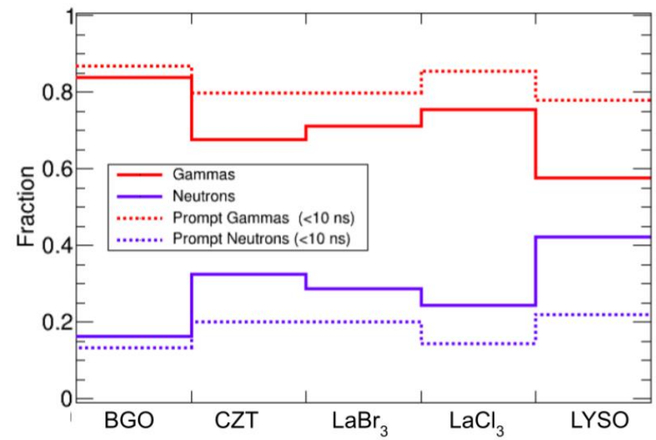

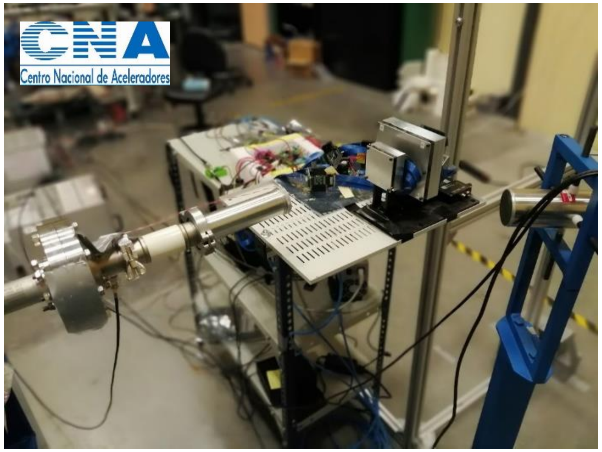

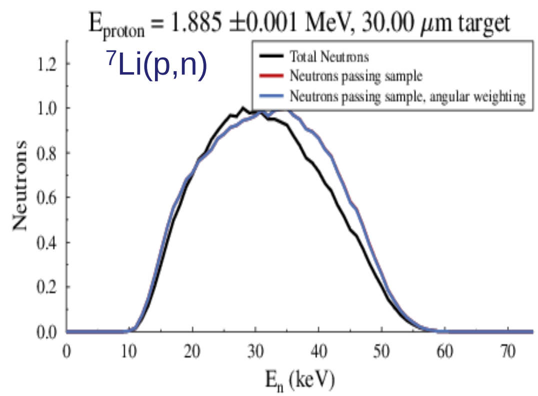

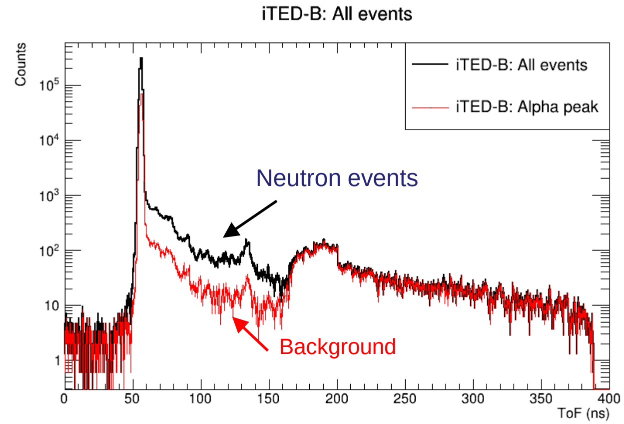

J. Lerendegui, J. Balibrea, et al. (CDP), Nat. Scientific Reports 2022

J. Lerendegui, et al. (CDP), NIM-A (in prep.)

Neutrons in HT: the role of a CC optimized for low neutron sensitivity

Nuclear Inst. and Methods in Physics Research, A 878 (2018) 58–73

Contents lists available at ScienceDirect

Nuclear Inst. and Methods in Physics Research, A

journal homepage: www.elsevier.com/locate/nima

ELSEVIER

Prompt-gamma monitoring in hadrontherapy: A review

J. Krimmer[a], D. Dauvergne[b,*], J.M. Létang[c], É. Testa[a]

[a] IPNL, Université de Lyon, Université Lyon 1, CNRS/IN2P3 UMR5822, F-69622 Villeurbanne, France
[b] LPSC, Université Grenoble-Alpes, CNRS/IN2P3 UMR5821, F-38026 Grenoble, France
[c] Univ Lyon, INSA-Lyon, Université Claude Bernard Lyon 1, UJM-Saint Étienne, CNRS, Inserm, Centre Léon Bérard, CREATIS UMR 5220 U1206, F-69373, Lyon, France

2.3. Specificity of PG imaging

Table 2 presents the specificities of PG cameras for hadrontherapy with respect to conventional medical imaging. It is clear from these specificities that dedicated cameras are needed, with special features like high energy detection capability and count rate capability, and data acquisition systems that have to be adapted to the beam time structure.

For the particular objective of the precision for the falloff determination in the 1D-profile, the background plays a major role. Indeed, if we describe the falloff features in terms of contrast C, falloff width FW and background level B, it has been shown that the falloff retrieval precision FRP is determined by the following equation for homogeneous targets [32]:

$$FRP = \frac{\sqrt{B}}{C} = \frac{1}{\sqrt{N}} \tag{1}$$

where N is the number of incident ions. A striking result is that the falloff width has no influence on the FRP. This means that the priority when optimizing camera designs is the detection efficiency and the background rejection (shielding, TOF,...).

As we will see in Section 4, detection efficiencies of PG cameras – ranging from 10^{-5} (collimated cameras) to 10^{-4} (Compton cameras) – will lead to relatively low numbers of detected PG at spot level for pencil beam scanning systems.

Precision for the falloff determination in 1D profile
C = contrast
FW = Falloff width
B = Background level

Falloff Retrieval Precision:
FRP = $B^{1/2}/C = 1/N^{1/2}$

[→ Falloff width has no impact →
(non Bragg-peak PGs and broad e+ distributions (PET) are ok)]

Key aspects of CC for PGI in HT:
- → Efficiency (→ i-TED array 4 CCs of large S.A.)
- → Background rejection (→ i-TED low Neutron Sensitivity)

Simultaneous Compton and PET imaging with i-TED in-situ in clinical conditions at HIT Heidelberg

Heidelberg Hadrontherapy Center

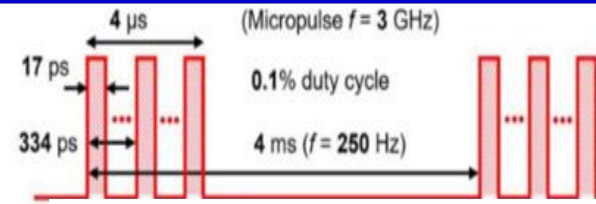

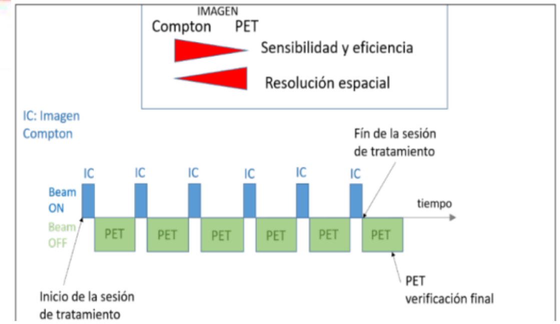

Compton 4x i-TED

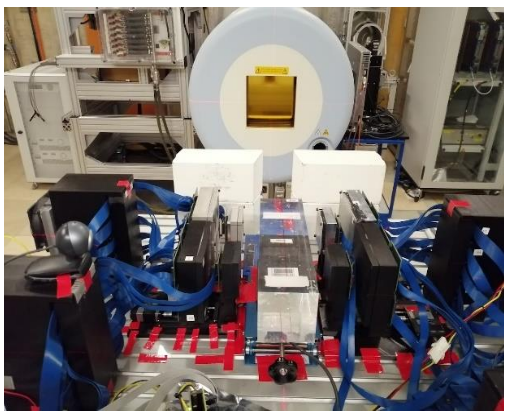

Compton & PET 4x i-TED

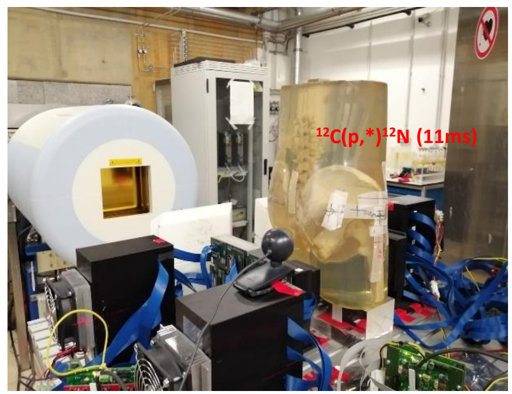

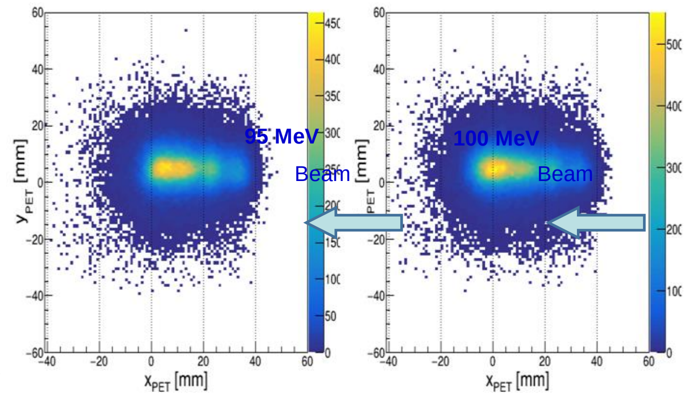

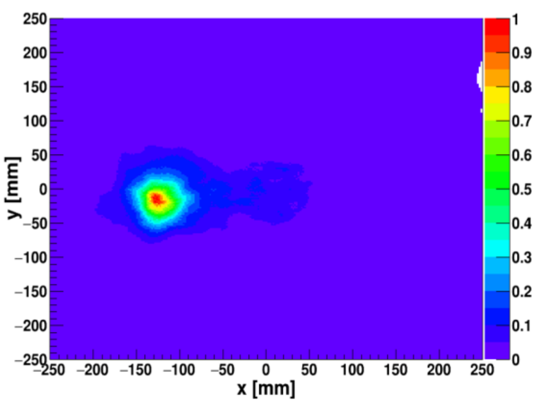

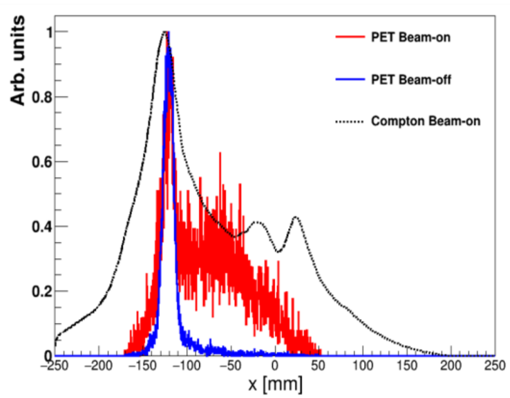

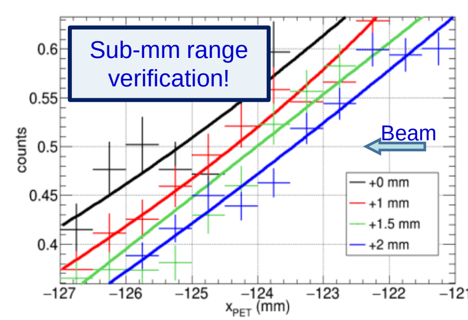

Latest upgrades: portability (wheels), adjustability (slider arms), new CPU